ELSEVIER

Tectonophysics 335 (2001) 229–253

TECTONOPHYSICS

www.elsevier.com/locate/tecto

New insights on 3-D plates interaction near Taiwan from tomography and tectonic implications

Serge Lallemand[a,*], Yvonne Font[b], Harmen Bijwaard[c,1], Honn Kao[d]

[a]*Laboratoire de Géophysique, Tectonique et Sédimentologie, UMR CNRS-UM2 5573, ISTEEM, Case 60, Place E. Bataillon, 34095 Montpellier, France*
[b]*Institute of Oceanography, National Taiwan University, P.O. Box 23-13, Taipei, Taiwan*
[c]*Vening Meinesz Research School of Geodynamics, Faculty of Earth Sciences, Utrecht University, P.O. Box 80021, 3508 TA, Utrecht, The Netherlands*
[d]*Institute of Earth Sciences, Academia Sinica, P.O. Box 1-55, Nankang, Taipei, Taiwan*

Received 20 September 2000; accepted 28 March 2001

Abstract

Recent tomographic results are used to trace the South China Sea and Philippine Sea subducting slabs, south and northeast of Taiwan along the Manila and Ryukyu trenches, respectively. In particular, the 3-D plates interaction beneath Taiwan is discussed based on a close-up view of the tomographic sections together with earthquake hypocenters distribution. Our study indicates that: (1) the east-dipping South China Sea slab can be followed to the north, up to the latitude of Hualien, (2) the Eurasian plate subducts beneath most part of the Taiwan island down to the 670 km-depth discontinuity, (3) the north-dipping Philippine Sea slab can be followed slightly west of the longitude of Hualien. Both plates thus interact beneath northern Taiwan where the arc–continent collision is paroxysmal. (4) Slab detachment is envisaged at the northern edge of the subducted Eurasian plate beneath the Coastal Range of Taiwan, which may facilitate the northwestward motion of the Philippine Sea plate with respect to Eurasia. Slabs geometries obtained from tomographic sections allow us to reconstruct the Late Neogene plate kinematics and dynamics in this region. Our main conclusions are: (1) The size of the original South China Sea was about twice its present size. (2) The subducted part of the West Philippine Basin i.e. the largest oceanic basin of the Philippine Sea Plate, extends only 400 km north of the Ryukyu Trench. (3) Slab detachment might have occurred 3–5 my ago beneath the central and northern Ryukyu Arc along a weak zone that is aligned with the Gagua Ridge: an ancient plate boundary. (4) The Ryukyu Trench has propagated westward from 126°E of longitude (southeast of Miyako Island) to the locus of the present arc–continent collision, along a major lithospheric tear that cut through the continent–ocean boundary first, and then through the continental lithosphere. As a consequence, the southern Ryukyu margin developed progressively from east to west as a subduction zone during the last 8 my. It has been elaborated onto a passive margin which corresponded to the edge of the Eurasian continental shelf bordering the South China Sea prior to Pliocene. (5) The Southern Okinawa Trough rifted during the last 2 ± 1 Ma following the propagation of the subduction zone. (6) Subduction of the Eurasian margin probably stopped recently beneath northern Taiwan and a flip of subduction from west to east is being initiated near Hualien.

Keywords: Taiwan; seismic tomography; trench–trench junction; subduction zone propagation

* Corresponding author. Fax: +33-4-67-52-39-08.
E-mail address: lallem@dstu.univ-montp2.fr (S. Lallemand).
[1] Present address: National Institute of Public Health and the Environment (RIVM), Laboratory of Radiation Research (LSO), P.O. Box 1, 3720 BA Bilthoven, The Netherlands.

0040-1951/01/$ - see front matter
PII: S0040-1951(01)00071-3

1. Introduction

This paper deals with the complex transition between two opposite verging subduction zones near Taiwan. A classical situation consists of a transform fault connecting both convergent boundaries, which is obviously not the case in Taiwan where arc–continent collision prevails. The knowledge of the initial plate configuration and the kinematic evolution are necessary prerequisites for anybody who aims to elucidate the present plate configuration. This is particularly true in the Taiwan region where the activity of the two merging subduction zones has been the subject of rapid and recent changes.

Available surface data provide an accurate 2D view of the active plate boundaries and deformed areas in the Taiwan region (Fig. 1). The submarine Manila Trench connects onshore to the north with the deformation front of the Taiwan mountain belt (Deffontaines et al., 1994; Liu et al., 1997; Mouthereau et al., 1999). In the same way, the Ryukyu Trench connects with the Longitudinal Valley Fault (e.g. Barrier, 1985; Lallemand et al., 1999). Both the Longitudinal Valley Fault and the deformation front are reported to be very active. Plate or structural block motions are estimated at the surface from geodesy and surface observations of active faults (e.g. Yu et al., 1997; Chamot-Rooke and Le Pichon, 1999; Imanishi et al., 1996; Angelier et al., 1997; Lee et al., 2001). The occurence of the Mw7.6 Chi-Chi earthquake on 21 September, 1999 near the deformation front has produced surface ruptures over a length of more than 80 km with both horizontal and vertical displacements up to 10 m (Ma et al., 1999; Kao and Chen, 2000). Our purpose is to extend surface informations in depth using geophysical imagery in order to provide a 3D view of the region.

What are the peculiarities inherent to the Taiwan area?

- Two opposite verging convergent plate boundaries intersect at right angle beneath Taiwan. The vergence change from an eastward dipping Eurasia (EUR) slab to a northward dipping Philippine Sea (PSP) slab occurs somewhere between Hualien and Taitung (Eastern Taiwan, see Fig. 1) with a complex interaction beneath the northern and central part of the island (e.g. Angelier, 1986; Teng, 1996; Lallemand et al., 1997a; Font et al., 1999).
- Both slabs subduct obliquely with respect to their NW/SE relative motion (Seno et al., 1993).
- Continental (Chinese platform) subduction beneath the PSP (northern extent of the Luzon Arc) is responsible for arc–continent collision (Angelier et al., 1986; Lin and Roecker, 1993; Malavieille et al., 1998, 2001).

In this context, the following questions remain:

- What is the geometry of the converging plates beneath Taiwan?
- What is the recent evolution of the junction between oceanic and continental subduction?
- How to interpret the gap of intermediate to deep seismicity beneath most of the island (north of 22°40′N, e.g. Wu et al., 1997; Kao et al., 2000)?
- How to interpret the strain pattern segmentation along the Ryukyu Arc (Kao and Chen, 1991; Kao et al., 1998), as well as the contorted SCS slab geometry of the Manila subduction zone (Rangin et al., 1999a)?
- How to account for the lack of arc volcanism younger than Quaternary in the southern Ryukyus (Shinjo, 1999; Wang et al., 1999)?

The purpose of this study is first to summarize previous studies for determining the recent activity of the two opposite verging subduction zones; second, trace the subducting slabs from global tomographic images (Bijwaard et al., 1998) and global hypocenters determinations of earthquakes (Engdahl et al., 1998) and third, propose a comprehensive 3D geodynamic interpretation of the junction area that accounts for the various observations.

2. Previous works

Is there a Eurasian slab beneath Taiwan?

Previous geodynamic models are controversial with regard to the existence of a Eurasian slab beneath Taiwan. Geological studies attest for the existence of a mountain belt that grew rapidly since Late Miocene or even less. Mountain building is generally considered to have propagated from north to south as a result of the obliquity between the trend of the

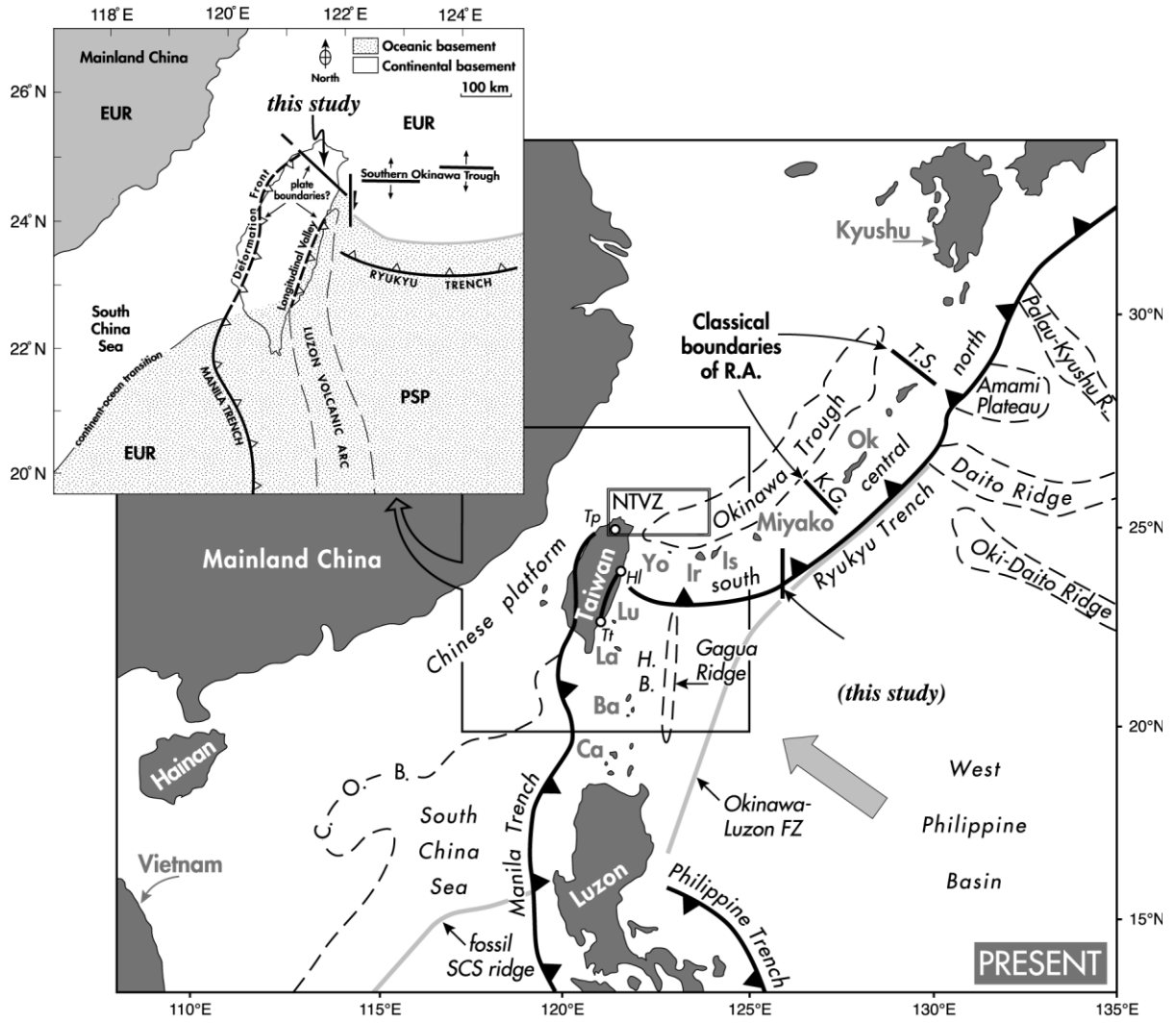

Fig. 1. Physiographic map of the Taiwan surroundings including the Ryukyu Arc and the northern Luzon Arc. T.S. = Tokara Strait, K.G. = Kerama Gap, Ok = Okinawa, Is = Ishigaki, Ir = Iri-Omote, Yo = Yonaguni, Lu = Lutao, La = Lanyu, Ba = Batan, Ca = Calayan, C.O.B. = continent–ocean boundary, Hl = Hualien, Tt = Taitung, Tp = Taipei. Insert: Geodynamic setting of the Taiwan region with the two active plate boundaries (longitudinal valley and deformation front) on both sides of the island and the surface projection of the tear fault that connects the deformation front with the Ryukyu Trench (this study).

backstop (Luzon volcanic Arc), those of the 'indenter' (talus of the Chinese passive margin) and the relative plate motion azimuth (e.g. Suppe, 1981). When restoring the plates before collision by extrapolation of present kinematics to the past, many geologists conclude that: (1) Taiwan results from the subduction of the Chinese continental platform beneath the PSP; (2) the SCS probably extended to the north and its oceanic domain should be subducted beneath Taiwan; and (3) a transform fault trending parallel to the relative plate motion might have existed between the two plates before collision to allow the change in polarity of subduction. In detail, the authors differ in the timing and the number of collision phases. Two 'collisional' mélanges: Kenting and Lichi, are observed in Taiwan but their ages are debated. Lu

and Hsu (1992) proposed a two-stage collision at 12 (Eurasia with Central Range associated with the formation of the Kenting mélange) and 3 Ma (Central Range with Coastal Range and formation of the Lichi mélange). Based on the analysis of nannoplankton (Chang and Chi, 1983) and planktonic foraminifera (Huang, 1984), two orogenic cycles have been distinguished from unconformities dated at 8 and 3 Ma in the western Foothills. Delcaillau et al. (1994) thus suggested a two-phase collision starting at 8 Ma instead of 12 Ma. Based on kinematic modeling, other authors consider a single arc–continent collision starting at 6.5 Ma for Huang et al. (1997), 6–4 Ma for Barrier and Angelier (1986), 5–3 Ma for Teng (1996), Mouthereau (2000), 4 Ma for Suppe (1984) or 3–2 Ma for Malavieille et al. (2001).

Earthquakes distribution (Wu, 1978; Tsai, 1986; Kao et al., 2000) or crustal velocities deduced from P- and S-wave tomography (Chen, 1995; Rau and Wu, 1995; Wu et al., 1997) provide constraints on the deep structure beneath Taiwan. Based on intraslab seismicity, the Benioff zone of the SCS can be identified down to about 140 km south of 23°N, at the latitude of Taitung. North of this latitude, no earthquakes have been recorded at more than 80 km depth. P-wave tomography obtained from seismic stations in Taiwan (Rau and Wu, 1995) indicates that the Moho depth increases from 25 km under the Western Foothills to 45 km under the Central Range to the east (see Section CC′ on Fig. 2). Moho's depth also increases from 40 km in the south (latitude of Taitung) to 55 km in the north (latitude of Taipei) along the Central Range. The 7.5 km/s velocity curve, that could represent the Moho, suddenly jumps north of 24°40′N from 55 to 35 km (Fig. 2, Section BB′). We will propose further in this paper a simple explanation for that observation. We interpret the low velocity zone, which deepens eastward beneath the Central Range along Section CC′, as the Taiwan orogen made of continental crustal slices offscraped from the subducting Eurasian plate. Deeper than 80 km, a high velocity anomaly (Vp and Vs), dipping about 50° east, has been imaged by Chen (1995) beneath the Coastal Range at 23.5°N. The anomaly could be interpreted as the continuation of the mantle part of the Eurasia slab. The controversy comes from the fact that there is no associated seismicity down to 60/70 km. Wu et al. (1989) thus, interpreted the low seismicity under the Central Range — except at depths between 60 and 80 km at 24°N latitude (Lin and Roecker, 1993) — as a change in rheology of continental upper mantle (ductile vs brittle behavior) caused by a high thermal gradient.

Based on earthquake data acquired from a local seismic network, Lin et al. (1998) suggested that the higher velocities and extensional mechanisms in the Eastern Central Range are caused by the ongoing exhumation of previously subducted continental crust, whereas the lower velocities to the west reflect continued underthrusting of the crust beneath the Eastern Central Range.

2.1. Activity of the Ryukyu subduction zone since Miocene

The Ryukyu subduction zone is generally described along three — almost equally long — segments separated by the Tokara Strait (between the Northern and Central segments) and the Kerama Gap (between the Central and the Southern segments). The subduction velocity, as well as the convergence obliquity increases southward with a change at the longitude of Miyako (the easternmost Yaeyama island at 125°30′E — Fig. 1). This rapid change is caused by the sharp variation in the trench/arc/backarc azimuth from NE–SW to E–W and the combination of the increasing PSP motion with respect to Eurasia (as a result of the increasing distance of the rotation pole; Seno et al., 1993) and the high rate of the southern Okinawa Trough opening (Imanishi et al., 1996). Near Taiwan, the convergence rate is about 8 cm/yr between the PSP and the Chinese continental margin (Yu et al., 1999) and 10.7 cm/yr between the PSP and the southernmost Ryukyu Arc (Lallemand and Liu, 1998).

The Ryukyu volcanic front is expressed in the north and becomes indistinct in the central and southern parts. A recent swath-bathymetric survey has shown that an embryo volcanic front may be expressed in the southern part of the southern Okinawa Trough (north of Yonaguni Island; Lallemand et al., 1997b). According to recent geochemical studies of volcanoes from the central and southern Ryukyu Arc, Shinjo (1999) stated that the appearance of high magnesian andesite magma at 13 Ma in Iriomote is obviously inconsistent with active subduction at that time. According to Shinjo (1999), this island should

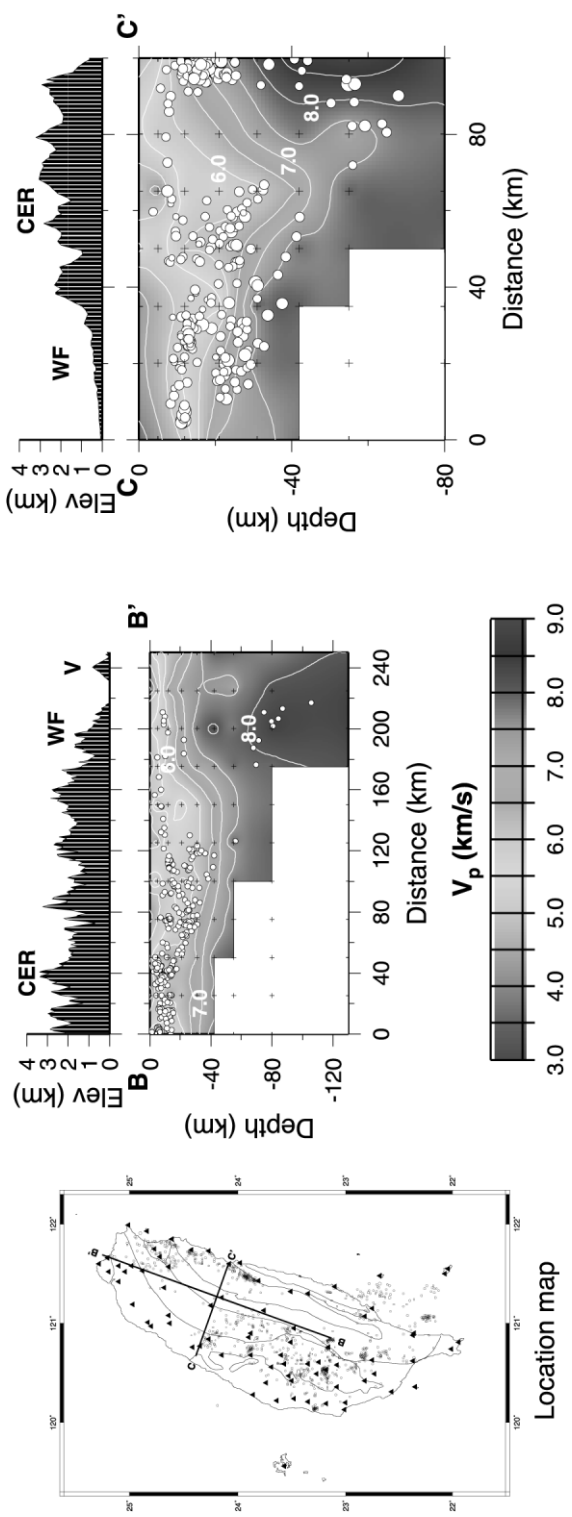

Fig. 2. Seismic P-wave tomography along two sections across Taiwan after Rau and Wu (1995). Velocity contour interval is 0.5 km/s. White circles are relocated earthquakes hypocenters. CER = Central Range; WF = Western Foothills; V = Tatun volcano.

represent the easternmost extent of Miocene intraplate magmatism. Furthermore, the absence of any subduction-related magmatic record from the Miocene to the Pliocene on the emerged Yaeyama islands suggests that the western part of southern Ryukyus was not a subduction zone in the Middle Miocene and that the arc–trench system was established after the collision of the Luzon Arc. In support with this hypothesis, Wang et al. (1999), after studying all the volcanoes from the northern Taiwan volcanic zone (NTVZ — Fig. 1), concluded that the southern Okinawa Trough (SOT) represents an atypical backarc basin that developed broadly synchronously with its arc–trench system. Based on the study of seismic reflection profiles acquired in the SOT, Park et al. (1998) concluded that back-arc rifting probably initiated during the early Pleistocene. The young volcanism from the NTVZ, varying from low-K to calc-alkaline and shoshonitic compositions, results from post-collisional lithospheric extension in the northern mountain belt. The oldest volcanic activity recorded in the Central Ryukyu volcanic arc has been dated Early Miocene (18 Ma; Kizaki, 1986; Shinjo, 1999), whereas the NTVZ began only at 2.8–2.5 Ma and lasted during the entire Quaternary (Wang et al., 1999). Volcanoes are sitting 200–250 km above the north-dipping Benioff zone of the PSP, except a chain of recent but undated seamounts that have been emplaced about 100–120 km above the subducting slab (Sibuet et al., 1998).

In most reconstructions, a tectono-magmatic event is recorded in the central and northern Ryukyu Arc during the Late Miocene. Shinjo (1999) noticed the absence of arc volcanism in the Ryukyus between 13 and 6 Ma. Several authors propose a change of motion of PSP (Seno and Maruyama, 1984; Huchon, 1986; Jolivet et al., 1989; Shimizu and Itaya, 1993) between 12 and 5 Ma which could be associated with arc–continent collisions (Luzon Arc in Taiwan, Palau–Kyushu Ridge and Izu–Bonin Arc in SW Japan).

The maximum depth of seismicity varies from 200 km beneath Kyushu to about 270 km near Taiwan (Katsumata and Sykes, 1969). The density of shallow and intermediate earthquakes increases drastically near Taiwan, partly as a result of ongoing arc–continent collision as attested by lateral compressional events (Kao et al., 1998; Kao and Rau, 1999).

2.2. Activity of the northern Luzon subduction zone

Uncertainties in dating the calc-alkaline volcanic rocks from northern Luzon to the Taiwan Coastal Range partially come from the assumptions made in K–Ar method. Yang et al. (1995, 1996) using the fission-track method provide a Plio-Quaternary age for most of the samples except in northern Luzon island (22 and 26 Ma) and in the northern Coastal Range (8–16 Ma). Juang and Bellon (1984), Richard et al. (1986), based on K–Ar method, have reported in the Coastal Range of Taiwan, Lutao and Lanyu islands ages as old as 30 Ma with apparent gaps between 17 and 23 Ma and 25 and 30 Ma. The oldest arc volcanism is thus Oligocene. To the opposite, the youngest volcanic activity in the northern part of the arc is 4 my old at the latitude of Hualien, 1.5 my old in the southern part of the Coastal Range, 0.5 my old in Lutao and 20 kyr in Hsiao–Lanyu (an islet close to Lanyu island). The progressive extinction of arc volcanism observed in the datings from north to south, is consistent with the diachronic 30° clockwise rotation of the Coastal Range deduced from paleomagnetism. Block rotations started between 3 and 4 Ma ago in the northern Coastal Range and then propagated southward at a speed of about 70 km/Ma (Lee et al., 1991). These rotations are in agreement with an arc–continent collision starting 4 Ma ago in the northern Coastal Range.

As said previously, the Benioff zone of the SCS slab is traced up to 23°N. No seismic events deeper than 70 km, and which could be linked with the SCS slab, are detected north of this latitude (Kao et al., 2000).

3. New insights from global tomography

We have seen from previous studies that both the southern Ryukyu and northern Luzon (Manila) subduction zones have encountered a complex evolution near Taiwan during the last millions of years. Relicts of past subducting slabs can be searched by the use of tomography, providing a key for better understanding of the Late Neogene tectonic evolution of the area.

A global model of seismic travel-time tomography has been published by Bijwaard et al. (1998). Because of its new subdivision of the Earth's mantle and crust

into irregular cells with sizes adapted to the amount of local seismic ray sampling, plate boundaries and especially subduction zones are well-resolved due to the concentration of earthquakes. In the studied area, lateral heterogeneities on scales as small as 0.6° are resolved in the upper mantle allowing us to map subducting slabs. The data used are a reprocessed version of the ISC (International Seismological Centre) data set supplemented with recent data from the USGS's NEIC (US Geological Survey's National Earthquake Information Center) and from temporary deployments of seismic stations (Engdahl et al., 1998). It comprises over 82,000 well-constrained earthquakes and a total of 12 million first- and later-arriving seismic phases observed in the period 1964–1995, from which Bijwaard et al. (1998) select 7.6 million teleseismic P, pP, and pwP data.

Spike tests were performed (similar to checker-board tests but in 3D) to assess the resolution of tomographic inversions in the studied area. We have used various sizes of spikes (0.6, 1.2, 1.8 and 2.4°) and made sections at 13 different depths between 18 and 710 km to avoid erroneous interpretations in terms of resolution that may result from the effect described in Lévêque et al. (1993). We only show the results obtained at four depths with two spikes sizes for each level (Fig. 3). Spikes are cut in half through their centers because it gives the best measure of resolution. That is the reason why the depth in the middle of spikes does not necessarily coincides with those of horizontal slices of the tomographic model. In any case, we are confident in the resolution even along vertical sections (continuity of slabs?), because patches are all in high hit count areas (most rays travel down-dip in subduction zones). The top layer is not resolved and its structure is absorbed by station corrections but the second layer (53 km) looks rather well with even some resolution for 0.6° spikes directly below the island. Resolution for 0.6° peaks is good down to 200 km, but for 1.2° peaks, it is even better from 53 to approximately 320 km. Below 320 km, resolution deteriorates to 1.8° for the rest of the upper mantle.

3.1. Cross-sectional views of the model from Kyushu to Luzon

We have made four sections across the Ryukyu Trench and three across the Manila Trench, down to 1500 km into the mantle from Kyushu to Luzon islands (Fig. 4). Velocity contrasts are ±1.5% for the entire cross-sections.

Section AA′ south of Kyushu clearly shows the PSP slab down to a depth of 300 km with its associated Benioff zone. A regional high-velocity area lies in the transition zone between 450 and 670 km that might be attributed either or both to the Pacific plate subducting beneath the Izu–Bonin Arc and/or to a former PSP slab that had been detached. The length of the slab which is still attached with the PSP is 450 km.

Section BB′ north of Okinawa island shows the seismically active PSP slab down to a depth of 300 km (total slab length is 420 km). A 100 km wide gap (low-velocity zone) exists between the dipping slab and a high-velocity anomaly lying above the 670 km discontinuity that could represent a detached part of the same slab, as well as an extension of the Pacific slab.

Section CC′ south of Okinawa island is almost identical to the previous one, except that the high-velocity zone lying on top of the 670 km discontinuity is less continuous. The PSP slab, still attached with the plate at the surface, is 360 km long and reaches a depth of 220 km. It is interrupted for about 80 km and a high-velocity structure, extending from 300 to 670 km seems to have been detached from the rest of slab.

Section DD′ across the Yaeyama islands shows a continuous slab down to a depth of about 580 km whereas the Benioff zone only extends down to 300 km. The high-velocity zone seems constricted at a depth of 250–300 km, but the Benioff zone extends through it. We thus assume that it is continuous from the surface down to 580 km. This section is very oblique with the trend of the subduction zone, so that the slab dip is steeper than it appears on the section.

Section EE′ across Taiwan is the most surprising one with respect to the previous studies. Indeed, it clearly shows an aseismic eastward dipping slab down to a depth of 670 km, which gives an estimated slab length of 830 km. This high-velocity zone seems not connected to the surface (upward termination at 70 km depth). Given that the existing tomographic results clearly show a low-velocity anomaly beneath the Central Range of Taiwan (i.e. Wu et al., 1997; Lin et al., 1998), we can say that our results are consistent with previous ones at shallow depths. Nevertheless, it

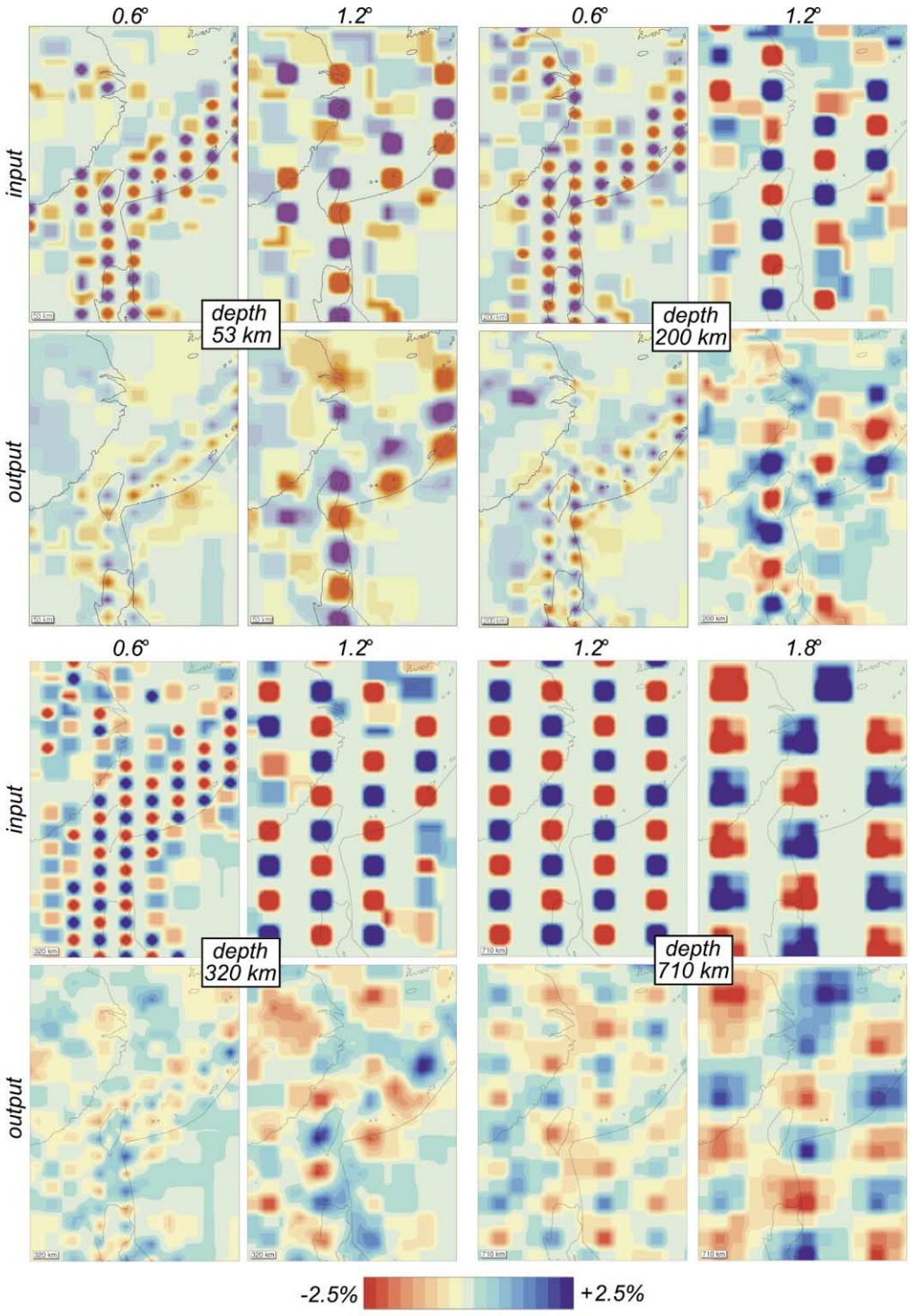

Fig. 3. Spike tests performed on the tomographic inversions for various depths: 53, 200, 320 and 710 km, and sizes of spikes: 0.6, 1.2 and 1.8°. Output image is shown below input one giving an estimate of the resolution of the tomographic model. The synthetic test area is comprised between latitudes 15 and 35°N and longitudes 115 and 130°E (NW quadrant of the area shown in Fig. 5). See the text for further explanations.

could also be an artifact of the poor resolution in the top layer because the high-velocity anomaly, which represents the SCS slab, does not reach at all the surface along the southern sections (see Sections FF′ and GG′). Another peculiarity is the steepness of the slab beneath Taiwan (EE′) and even more at latitude 20°N (FF′).

Section FF′ north of Luzon indicates a vertical SCS slab which could be overturned beneath the SCS itself in the transition zone. It is noticeable to observe that the subducting slab is aseismic below 250 km depth. Again, the slab seems disconnected with the surface (upward termination at 100 km depth). A conservative length of the vertically dipping slab is 880 km, but if we accept that it is overturned and thus continuous, then its total length reaches 1180 km. Another high-velocity zone lies in the transition zone, east of Luzon, which could connect with those observed in previous northern sections (Pacific remnant slab?).

Section GG′ across northern Luzon is significantly different from Section FF′ despite its proximity. Indeed, the SCS slab dips shallowly eastward until it reaches a depth of about 300 km. Again, intraslab seismicity is observed only at shallow depths and it seems disconnected with the surface (upward termination at 70 km depth). Its estimated length is 660 km from the trench.

3.2. Map views of the model from Kyushu to Luzon

Map views of the global model for the whole PSP area at depths of 100, 150, 200, 250, 300, 350, 400, 450, 500, 550, 600, 650, 700 and 750 km provide the third dimension for our interpretations (Fig. 5). Velocity contrasts are 2% for the upper 200 km, 1.5% between 200 and 650 km, and only 1.0% for the lower mantle (regions deeper than 650 km). We have picked the top of the supposed slabs on each vertical section (with question marks when the slab extent was ambiguous) and extrapolate the depths into contours using horizontal sections. Then, we have restored the slabs to their horizontal position before subduction by unfolding them, normal to the trenches. We finally obtain two pictures: one representing the PSP (Fig. 6a) and the other representing the SCS (Fig. 6b) with their respective subducted slabs projected onto the surface.

The PSP slab can be followed beneath the Ryukyus between Kyushu to the north and northern Taiwan to the south. It is well expressed and continuous from the surface down to a depth of 250 ± 50 km (Fig. 5). At higher depths (350 ± 50 km), a gap (low-velocity zone) appears beneath the central and northern Ryukyu Arc (see Fig. 4, Sections AA′, BB′ and CC′). Then, the slab appears continuous again at depths higher than 400 km with a possible extent toward the northwest near 27–28°N as shown on the unfolded PSP slab of Fig. 6a. The slab is apparently detaching along a direction parallel to the Ryukyu Trench (gray strip D1 on Fig. 6a) except in the southernmost part close to Taiwan.

The SCS slab is continuous from northern Taiwan to Luzon at depths between 200 and 250 km, even if a left-lateral offset by about 50–100 km occurs at latitude 21°N (immediately south of Taiwan). It is more irregular at depths shallower than 200 km and seems discontinuous also near 21°N. Deeper than 250 km, the SCS slab is only observed north of Luzon and could be overturned south of Taiwan below 450 km. The SCS slab extends up to the latitude of northern Taiwan until it reaches 500 km depth, then it disappears progressively from the north. The limb with the question mark on Fig. 6b outlines the possible overturned extent of the SCS slab (see Section FF′ on Fig. 4).

The junction between the two opposite verging SCS and PSP slabs occurs just north of Hualien at depths 100–250 km. They tend to separate below than 250 km.

3.3. Discussion on tomographic results

Only the shallow part of both slabs is seismic, which means that determining the slab extent only from the Benioff zone is not valid. The SCS slab is less seismic than the PSP slab, in particular beneath Taiwan. This aseismic behavior may be caused by several factors: (1) the SCS is a young back-arc basin (32–15 Ma; Taylor and Hayes, 1983) and the subducting plate was probably hot at the time of its subduction, especially near the fossil ridge, which is today located at the latitude of Luzon (see Fig. 1), but which has subducted north of Luzon in the past. It is generally observed that subduction of very young lithosphere (age <15–25 Ma) with high heat-flow (>75 mW/m^2) produces mainly shallow earthquakes

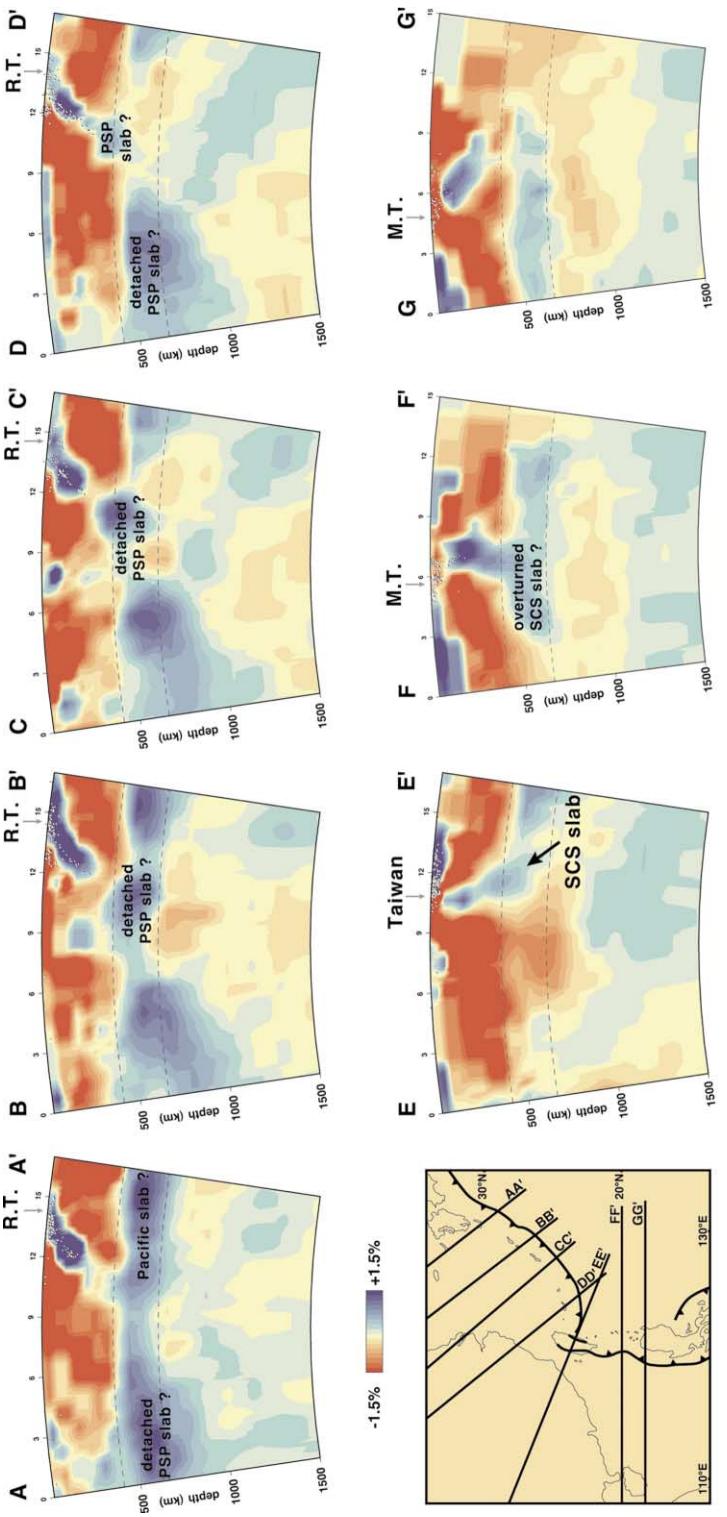

Fig. 4. Tomographic results displayed in seven vertical Sections AA′ to EE′ along the lines indicated in the map (lower left corner), showing the P-wave velocity anomalies under the northwestern margin of the PSP from the global model of Bijwaard et al. (1998). Velocity anomalies are displayed in percentages (±1.5%) with respect to the average P-wave velocity at depth. White dots are earthquakes. Blue denotes high-velocity zones and red low-velocity ones. R.T. = Ryukyu Trench; M.T. = Manila Trench.

(Kirby et al., 1996); (2) the two northern Sections EE′ and FF′ (Fig. 4) show a steep or possibly overturned slab, which might indicate that it became ductile after saturation of the bending moment; and (3) its tomographic image (high-velocity anomaly) vanishes and it seems offset to the north suggesting a possible detachment from the north propagating to the south at depths less than 100 km. Such detachment was also suggested by the P- and S-wave tomography performed beneath Taiwan by Chen (1995). The slab is lying just beneath eastern Taiwan rather than beneath the Huatung Basin as expected for a continuous slab. This is also in favor of a detached part, sinking into the mantle, whereas Taiwan is moving to the east with respect to Eurasia at a rate of about 2 cm/yr as evidenced by GEODYSSEA GPS results (Chamot-Rooke and Le Pichon, 1999; Rangin et al., 1999b). These authors assume that Taiwan belongs to the 'Sundaland block' behaving rigidly. Without detachment, such torque would be responsible for the overturned slab as observed along Section FF′ (Fig. 4; Rangin et al., 1999a).

Rangin et al. (1999a) estimated the length of the subducted part of the SCS at about 800 km near 20°N of latitude. Based on the map views, we can estimate the approximate length of the SCS slab from north to south. It quickly increases from 0 to 800 km between 25 and 23°N, then to 800–900 km (or even more when considering the possible overturned part of the slab) near 20°N with a rapid decrease between 19 and 18°N to 300 km at the latitude of 13°N.

The unfolded and horizontally projected PSP and SCS slabs with respect to the respective trenches (Fig. 6) allow us to make the following comments:

- The subducted part of the SCS Basin appears more or less equal in size with the present SCS. Its northern margin extended until 126–127°E of longitude (south of Miyako island, see Fig. 1), which means that the Yaeyama islands (Yo, Ir and Is on Fig. 1) were in the position of a passive margin prior to Late Miocene. This result is in excellent agreement with the observations by Shinjo (1999), Wang et al. (1999), based on the lack of earlier arc magmatism, who concluded that the southern Ryukyu subduction zone was active since Late Miocene or even Pliocene.
- The Ryukyu subduction zone has propagated westward from longitude 126–127°E first along the continent–ocean boundary (COB), and then across the continental Eurasian lithosphere, to finally reach its present termination beneath northern Taiwan as revealed by the reconstructions (T1 on Fig. 6). The subducted trace of the COB is uncertain as indicated by the question mark on Fig. 6b. All the emerged terranes have the same location than today (in pale gray on Fig. 6), except the southern Ryukyu islands (from Miyako to Yonaguni) which have been shifted 80 km to the north on Fig. 6b in order to avoid overlap between the subducted northern edge of the SCS and the southern Ryukyu margin. As a consequence, rifting of the Southern Okinawa Trough (SOT) probably followed soon after the westward propagation of the Ryukyu Trench.
- The western edge of the subducted part of the PSP aligns along 121°30′E of longitude, at least until 27°N on the unfolded PSP of Fig. 6a. Given that the present (and recent) motion of the PSP occurred toward the NW with respect to Eurasia, it means that there was no slab beneath the southern Ryukyus prior to Late Miocene. It also means that the Luzon Arc extended at least 400 km to the north of the Coastal Range and has been subducted (or accreted along the southern Ryukyu margin).
- The elongated gap in the PSP slab (D1) parallels the most prominent fracture zone (FZ) of the West Philippine Basin which presently follows the central Ryukyu Trench, i.e. the Okinawa–Luzon FZ (Okino et al., 1999, see Fig. 1). Its southern end, close to Yonaguni and Iri-Omote islands (Fig. 6a), suggests that it could be connected with the subducted northern extent of the Gagua Ridge which separates the Eo-Oligocene West Philippine Basin (WPB) from the Early Cretaceous Huatung Basin (see Fig. 1 for location; Deschamps et al., 2000). If the Gagua Ridge and D1 are connected, then the detachment occured along a weak suture zone between the Paleogene WPB and the subducted extension of the older Huatung Basin.

We will present an evolutionary model of plate convergence taking into account the supposed recent kinematics of the PSP and SE Asia in the last section,

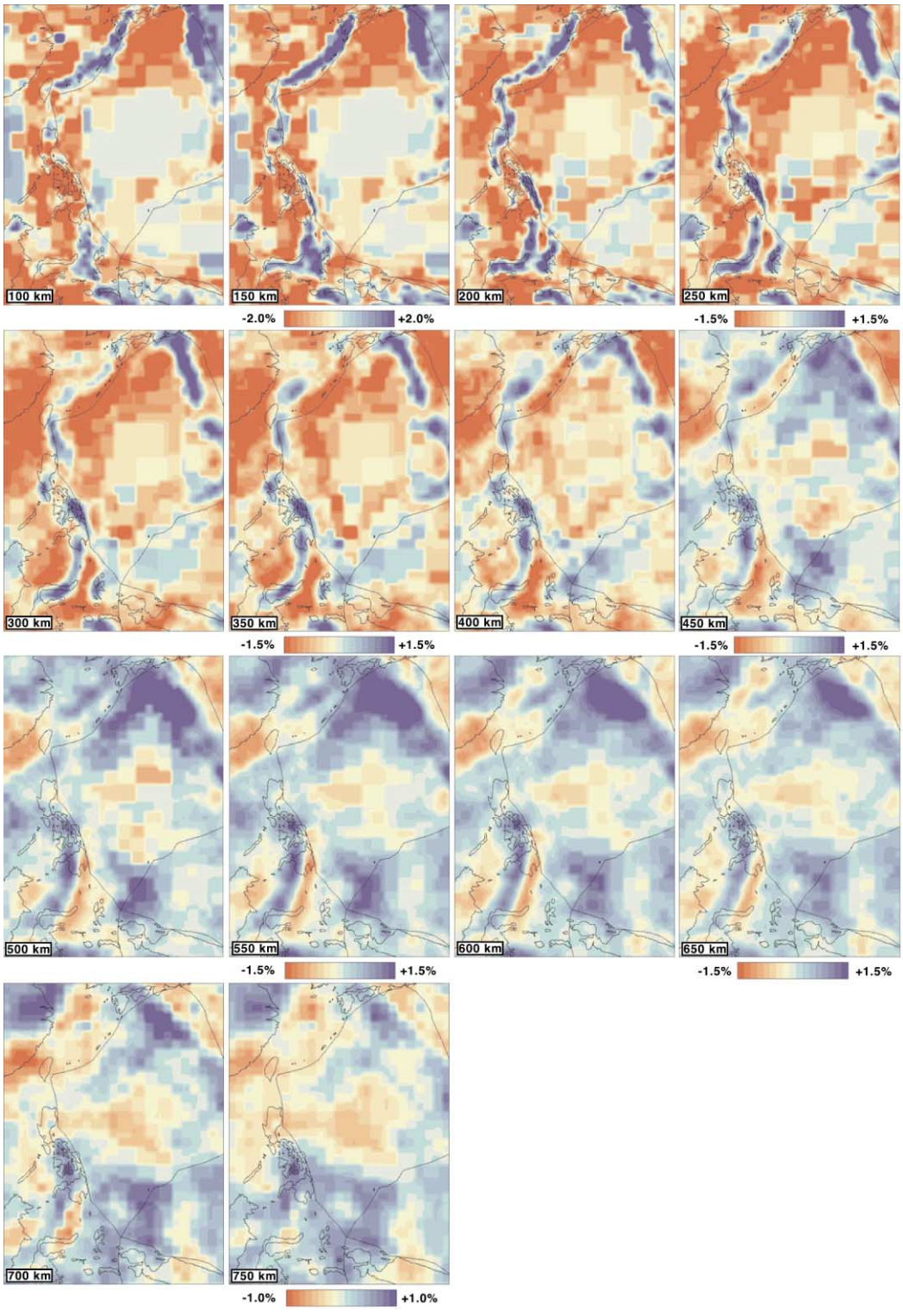
100 km
150 km
200 km
250 km
-2.0%
+2.0%
-1.5%
+1.5%
300 km
350 km
400 km
450 km
-1.5%
+1.5%
-1.5%
+1.5%
500 km
550 km
600 km
650 km
-1.5%
+1.5%
-1.5%
+1.5%
700 km
750 km
-1.0%
+1.0%

but we shall first compare the previous results to the seismicity pattern along these plate boundaries.

4. Seismological constraints

The number and magnitude of earthquakes increase drastically in the southern Ryukyu subduction zone west of 123°E (e.g. Wu, 1978; Tsai, 1986). It exists a clear NW–SE trend in earthquakes distribution in the Ryukyu forearc region between 121°30′E and 123°E at depths shallower than 60 km (Kao et al., 1998; see convergent arrows on Fig. 7), that aligns with the supposed boundary between the subducting part of the Eurasia plate and the non-subducting one (i.e. northernmost Taiwan and southermost Ryukyu Arc, see T1 Fig. 6b). Kao et al. (1998) interpreted some of these events as defining a lateral compression seismic zone, with a P-axis in the direction of the strike, within the subducting PSP caused by the nearby arc–continent collision. They interpreted another group of earthquakes in the same NW–SE swarm as defining the interface seismogenic zone with low-angle thrust faulting dipping north, whereas Font et al. (1999) interpreted the same group of earthquakes as defining a subvertical tear fault within the subducting PSP. The poor location of hypocenters in this area is responsible for this controversy and efforts are presently made for precise relocation of earthquakes in this particular area. We have used in this study (Fig. 7) the hypocenters of 1964–1995 $M_b > 4$ teleseismic earthquakes, from ISC and NEIC catalogs, relocated by Engdahl et al. (1998).

We present three sections (XX′, YY′ and ZZ′ on Figs. 7 and 8) across the most seismogenic area, perpendicular to the supposed NW–SE tear that cuts the Eurasia plate into a subducting part and a non-subducting one (T1 on Fig. 6b). The distance between the lines is 40 km, which is also the width of earthquake sampling (20 km on both sides of the lines). Hypocenters are used to adjust the plate contours, but the interpretation mainly comes from geological observations at shallow depths and spatial/geometrical considerations at greater depths

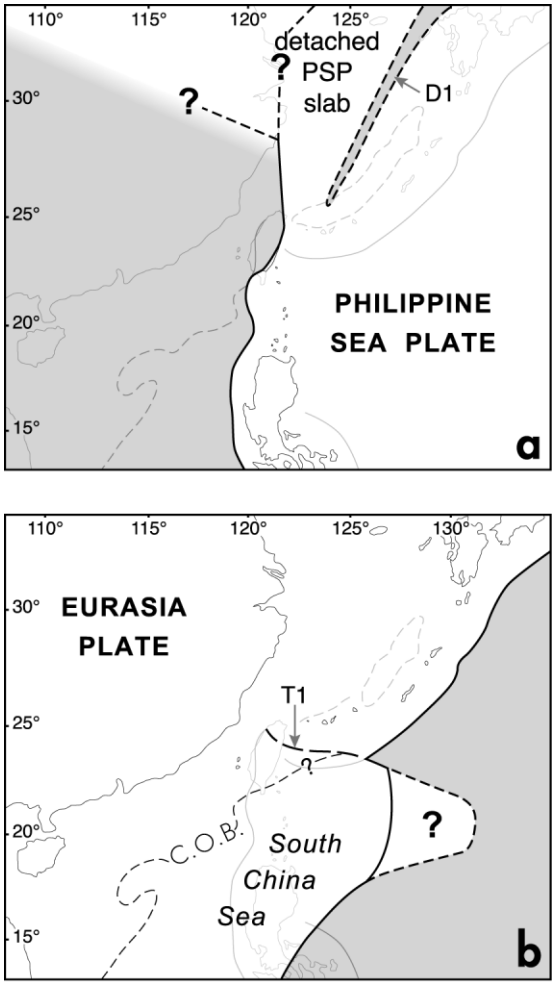

Fig. 6. Projection onto the surface of the (a) unfolded PSP slab; and (b) SCS slab; with some uncertainties (?) inherent to the resolution of the tomographic model at depth. C.O.B. = continent–ocean boundary. T1 = Tear fault n°1. See the text for explanations on the picking of the slab contours from velocity anomalies.

that are required for reconstructions. We know for example, from the recent Chi-Chi earthquake, that the orogenic deformation beneath the Foothills can reach down to 20 or even 30 km depth (Kao and Chen, 2000). We also know, from detailed reflection seismic studies (Font et al., 2001), that the Ryukyu

Fig. 5. Tomographic results displayed in 14 horizontal sections at depths from 100 to 750 km in the mantle beneath the whole PSP and its surroundings from the global model of Bijwaard et al. (1998). Velocity anomalies are displayed in percentages varying from 2 to 1% with respect to the average P-wave velocity at depth. The area is comprised between latitudes −5 and 35°N and longitudes 115 and 145°E.

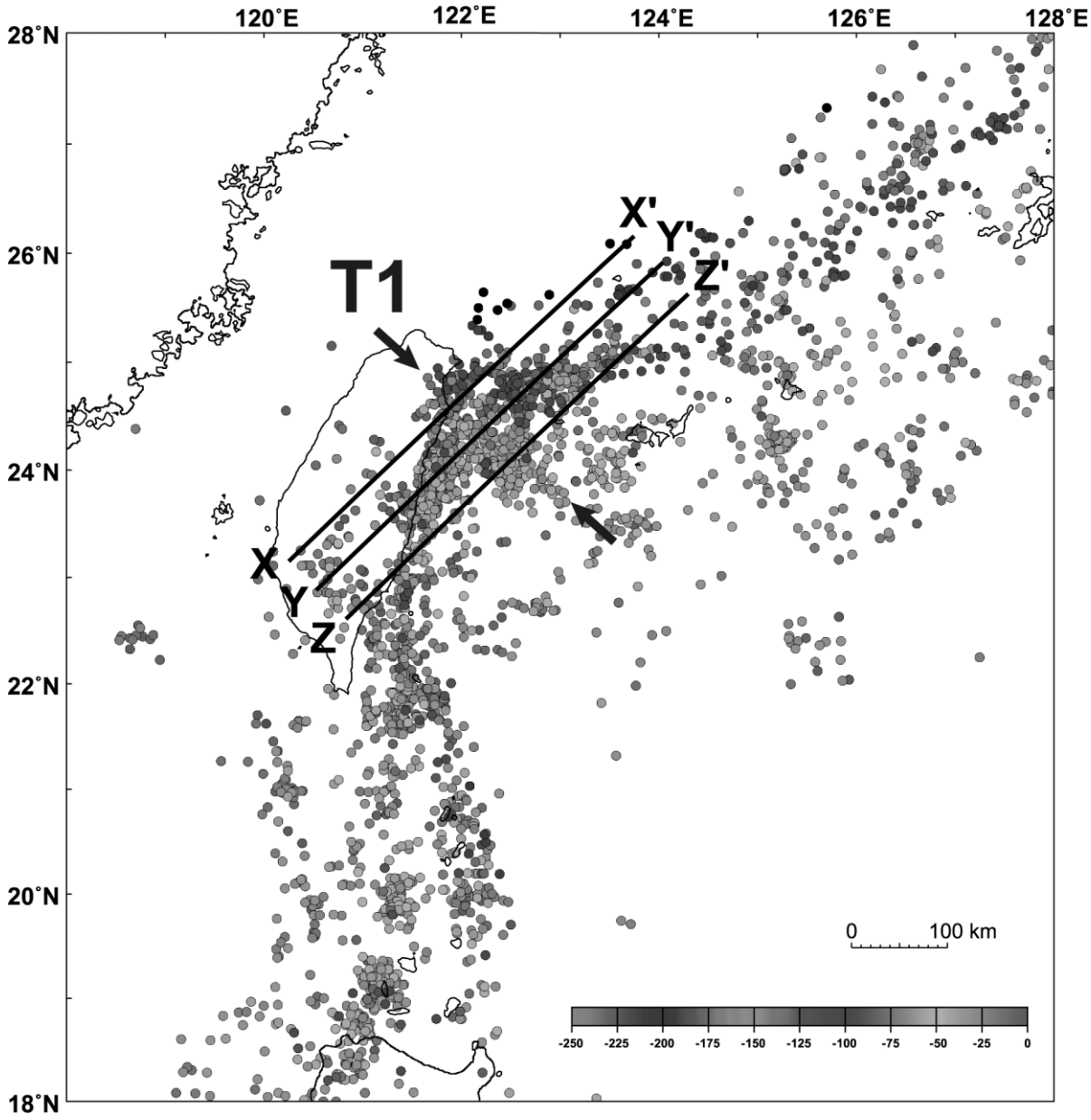

Fig. 7. Map of $M_b > 4$ earthquakes epicenters around Taiwan extracted from Engdahl et al. (1998) 1964–1995 data set. All events are well-constrained teleseismic earthquakes reported to the International Seismological Centre (ISC) and to the US Geological Survey's National Earthquake Information Center (NEIC) that were relocated by the authors. The three Sections XX′, YY′ and ZZ′ of Fig. 8, 500 km long, are located with ticks every 10 km. Note the concentration of earthquakes northeast of Taiwan. The convergent arrows indicate the trend of T1.

Arc basement ends abruptly along a vertical wall, more than 5 km high, located beneath the rear of the accretionary wedge. The location of SOT axis, transcurrent faults and thrust faults in the collision area are reported from the recent ACT survey (Lallemand et al., 1997b, 1999). A tear fault (T2), with a small vertical offset, is indicated with a question mark within the subducting PSP as proposed by Lallemand et al. (1997a), but its existence is not crucial for the purpose of this study. Based on tomographic data, a slab detachment (D2) is suggested, by a downward arrow on Fig. 8, at the termination of the subducting EUR plate. If it occurs, the detachment plane should be cut very obliquely by XX′, YY′ and ZZ′ sections.

The major point in these seismological sections is the break that affect the Eurasia plate along the vertical tear T1 into which the PSP inserts. Only the northern Luzon volcanic arc (L.A. on Fig. 8) is inserted along Sections XX′ and YY′, but moving south, the oceanic crust of the Huatung Basin is progressively sandwiched between the two edges of the EUR plate (Section ZZ′ on Fig. 8). The cartoon on Fig. 9a shows the SCS just before its subduction a few my ago. The basin was part of the EUR plate and it consisted of an oceanic (gray) and a continental (white) domain separated by a continent–ocean boundary (COB). The tear (T1) has first propagated westward along the COB and then northwestward through the continental lithosphere as sketched on Fig. 9b. This allowed the southern part of EUR to subduct, creating a gap that is filled by the PSP moving northwestward (Fig. 9c). The deformation of the Luzon arc is probably very intense, as shown by the high level of seismicity beneath Hualien in Fig. 8

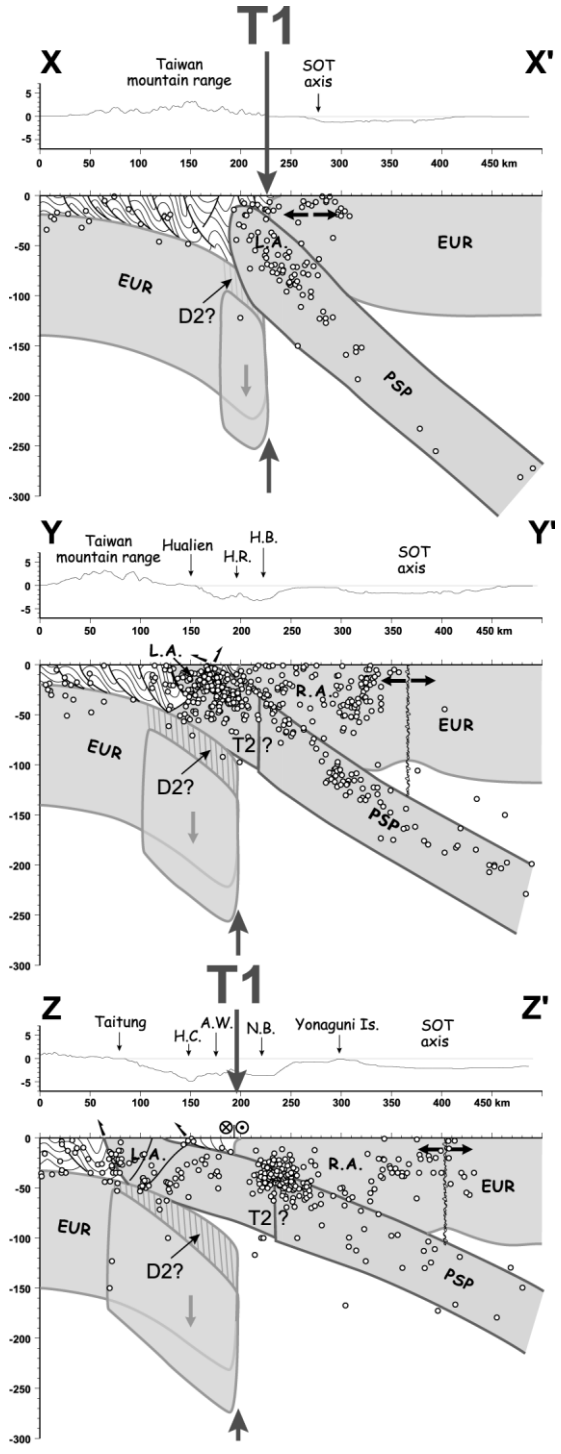

Fig. 8. Three SW–NE interpreted seismological sections across the major tear T1 that cuts the EUR plate, giving space for the PSP to propagate westward. The topography and toponymy is reported above each section with a vertical exaggeration of 5. Hypocenters are extracted from Engdahl et al.'s data set (1998) and sampled over a band 20 km wide on both side of the line (40 km wide total). See Fig. 7 for lines location. EUR = Eurasia plate; PSP = Philippine Sea plate; R.A. = Ryukyu Arc; SOT = Southern Okinawa Trough; H.R. = Hsincheng Ridge; H.B. = Hoping Basin; H.C. = Hualien Canyon; A.W. = accretionary wedge; N.B. = Nanao Basin; T1 and T2 are tear faults, D2 indicates a slab detachment with part of the EUR plate sinking into the mantle. The interpretation has been oversimplified for clarity matters but the Luzon Arc (coastal range) is probably heavily deformed by collision as well as the Ryukyu Arc.

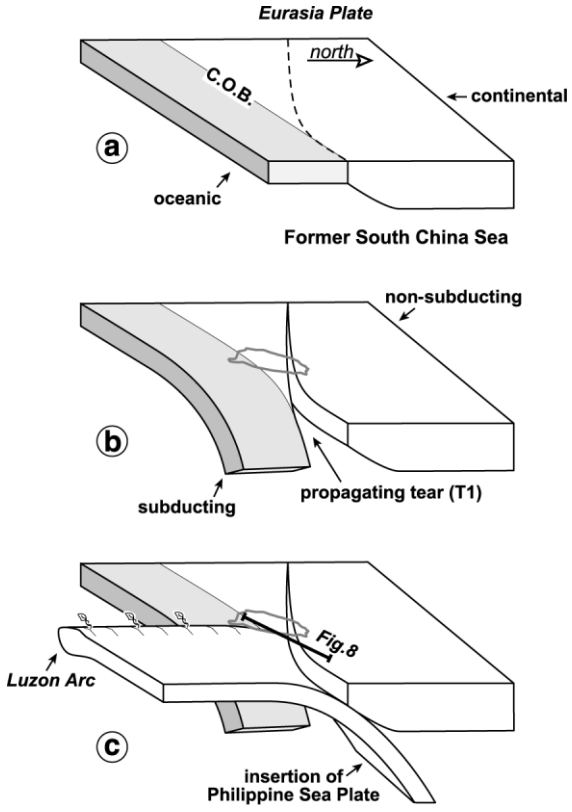

Fig. 9. (a) Sketch illustrating the tear T1 within the Eurasia plate (EUR), starting along the continent–ocean boundary (COB) and then propagating into the continent. (b) The vertical motion along the tear allows the southern part of EUR to subduct whereas the northern part does not. At first, only the oceanic domain of the SCS is subducting, but progressively a triangle of continent is also involved in the subduction. The subduction of the continental part of EUR marks the onset of arc–continent collision in Taiwan. The PSP is not represented in (a) and (b), but of course the PSP inserts within and subducts beneath the EUR concomitantly with the tearing of EUR as shown in (c). In detail, the SCS slab is much steeper than presented as shown on Fig. 10.

(Section YY′). Strong deformation is also expected in the frontal part of the Ryukyu Arc basement, because it has to shape progressively into a wedge together with the oblique insertion of the PSP in between the vertical walls of the tear fault plane, as shown by the concentration of earthquakes near the plate interface beneath the Nanao Basin in Fig. 8 (Section ZZ′).

The subducting part of the EUR plate shows very scarce seismicity, as previously noticed by many authors (e.g. Wu et al., 1997), but its existence is required from geometrical reasons as illustrated on Fig. 9b, and attested by tomographic sections (Section EE′ on Fig. 4). The tomographic section illustrated on Fig. 2 (Section BB′ of Rau and Wu, 1995) can now be explained by the plate geometry shown on XX′ (Fig. 8).

5. Discussion

5.1. 3D geometry of plates interaction beneath Taiwan

Because the same EUR plate subducts beneath Taiwan and overrides the PSP plate along the Ryukyu Arc, it must tear along T1 with a northwest propagation rate that should equal the convergence rate. The complex 3D interaction between the two converging plates in the vicinity of Taiwan is better explained when sediments (Taiwan mountain belt, Ryukyu forearc basins and accretionary wedge) are removed (Fig. 10). The SCS slab could be detached beneath Taiwan (D2) as a result of the strong E–W compressive stress exerted by the subducting PSP slab. In a recent paper, Kao and Jian (2001) described an arc–continent collision in southern and central Taiwan changing into a ‘slab-continent collision’ beneath northern Taiwan. The subducted trace of the COB could be inferred from geological observations on the starting time of arc–continent collision (see the debate in Section 2), knowing the convergence rate. The continuity of T1 has certainly been disrupted by the southward drift of the southern Ryukyu Arc that occur after its propagation (Lallemand and Liu, 1998). A strong deformation of the southern Ryukyu Arc basement is expected soon after the propagation of T1 because the newly formed active margin must necessarily shapes from a subvertical wall (if the tear fault is vertical) into a wedge. This should explain the intense seismic activity in the region and the difficulty that most seismologists have to provide a simple velocity structure of the margin (e.g. Wang and Chiang, 1998; McIntosh and Nakamura, 1998).

5.2. Additional constraints on the extension of T1

The southernmost Ryukyu forearc basement ends abruptly beneath the rear of the accretionary wedge

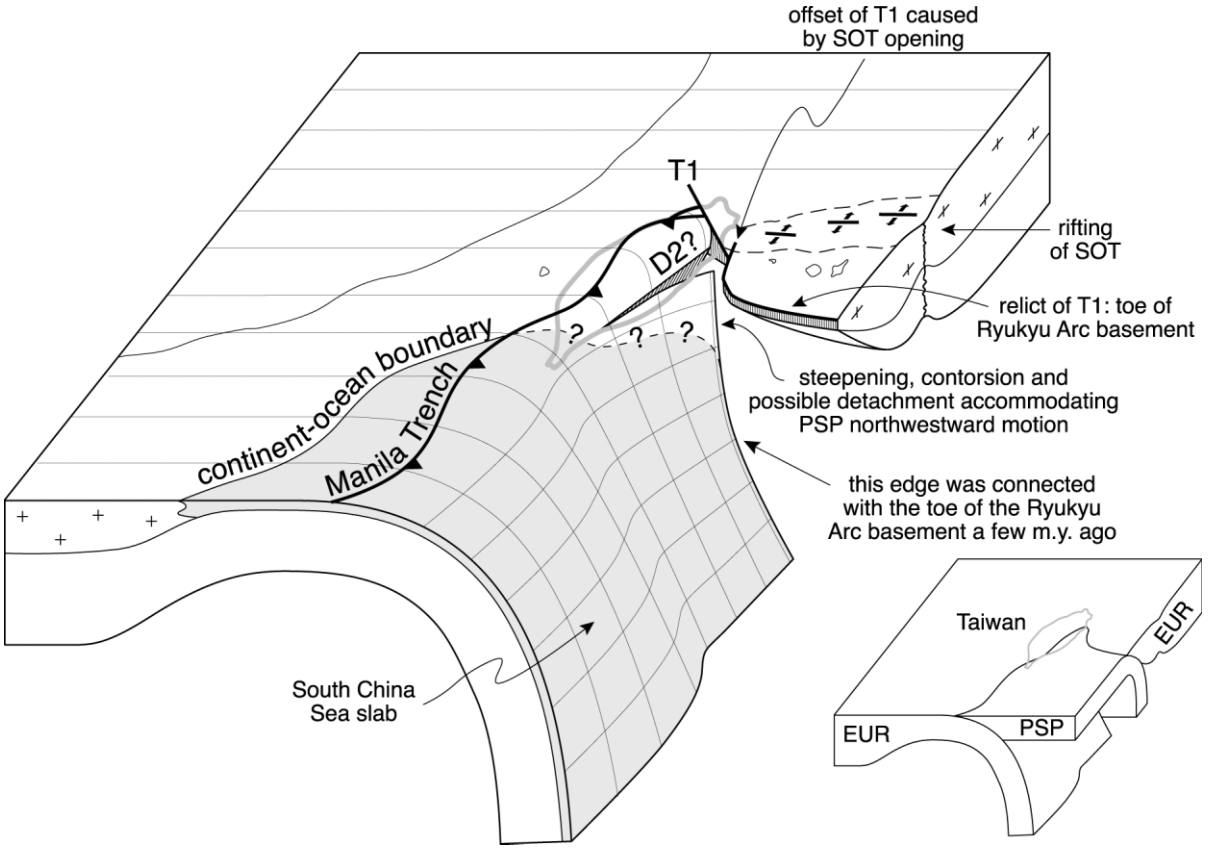

Fig. 10. 3D perspective view of plates interaction beneath Taiwan based on tomography, hypocenters distribution and geodynamics of the area. The dark gray represents the oceanic part of the Eurasia Plate (SCS). The transition between continent and ocean is noted C.O.B. The PSP has been removed for a better understanding of the geometry of the EUR plate in depth. All the sediments are removed and only the basements of the plates are represented on this figure. T1 is a tear fault cutting through EUR lithosphere and D2 is a possible detachment within the same EUR lithosphere. The cartoon in the bottom-right corner illustrates the same picture with the interacting PSP.

(Font et al., 2001). This major discontinuity, which represents the northern fault wall of T1, has certainly served as a guide for the major E–W transcurrent fault that cuts through the forearc (Lallemand et al., 1999). Dominguez et al. (1998) argued that the accretionary wedge is transported westward with respect to the Ryukyu Arc at a rate near 4 cm/yr along the fault. This major linear transcurrent feature is observed over a distance of about 450 km east of Taiwan as seen on detailed bathymetric maps (Matsumoto et al., 1993; Hsu et al., 1996). The morphology and strike of the Ryukyu forearc area change drastically near 126°E of longitude, from an E–W trend near Taiwan to a NE–SW direction along the rest of the arc (Fig. 1).

Our model supposes the termination of T1 offshore NW Taiwan in the Taiwan Strait, which is apparently not supported by the occurrence of historical earthquakes. Nevertheless, one may observe that a low free-air anomaly is followed from the Manila Trench up to 25°N (Hsu et al., 1998) marking the flexure of EUR under the load of the mountain range, in agreement with continental subduction until the latitude of Taipei (Fig. 11). Yu and Chou (2001) provide a detailed description of the western Taiwan foreland basin filling the flexural trough and extending up to 25°20′N of latitude. The convergent arrows on Fig. 11 mark the termination of the flexural trough as well as the sharp gravity gradient between high anomalies

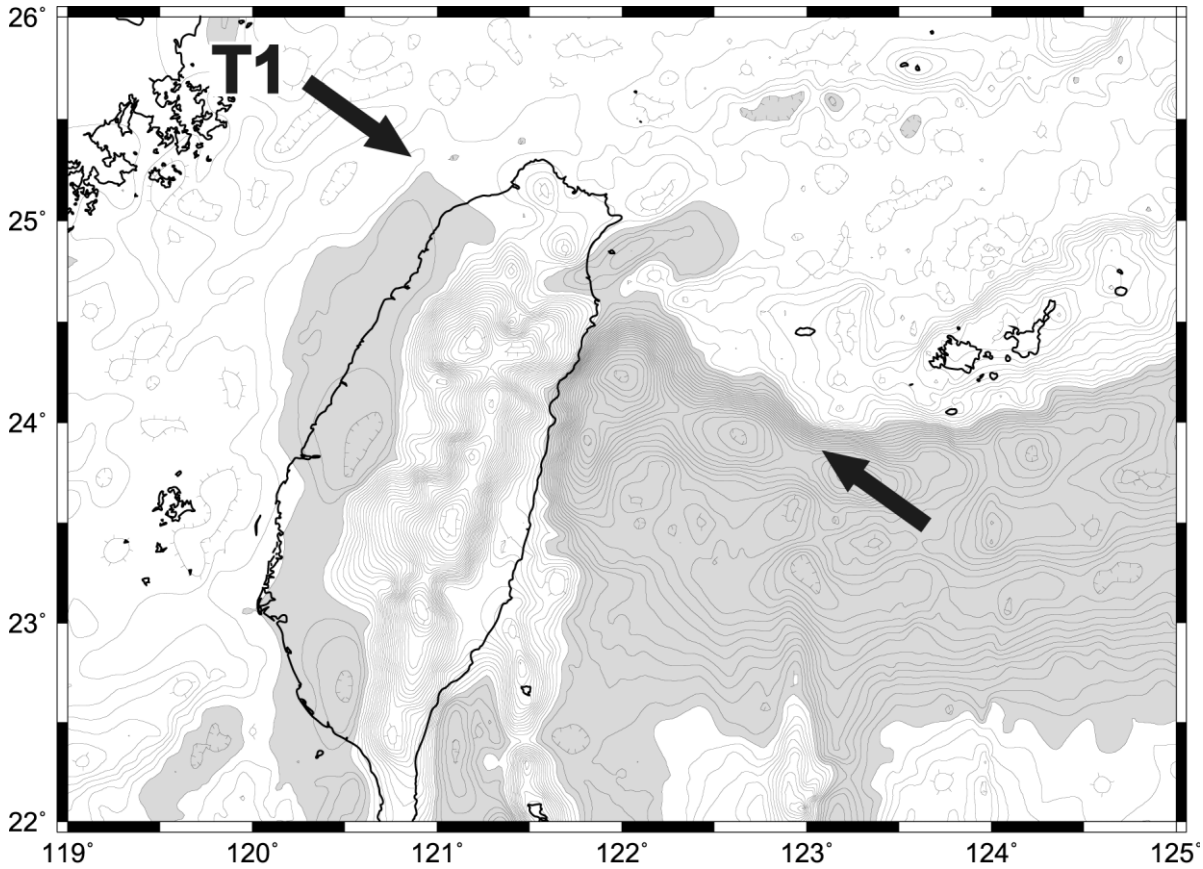

Fig. 11. Free-air gravity anomaly from Hsu et al. (1998) with contours every 10 mGals. Gray pattern reperesents negative anomalies. The convergent arrows indicate the possible trend of T1 marked by a sharp gravity gradient.

in the Central Range to the south and low ones to the north. We believe that this trend in gravity coincides with the continuation of T1, which is buried beneath the deformed orogen.

We thus observe an excellent agreement between the trace of T1 deduced from the projection of the SCS slab onto the surface (Fig. 6b) and the prominent transcurrent feature which characterizes the southern Ryukyu forearc between 122 and 126°E. Surface expression of T1 is less clear near Taiwan because it is overprinted by the recent tectonic movements associated with the SOT rifting and the forward development of the orogen. Nevertheless, we use the NW–SE strong gravity gradient across northern Taiwan as an indicator of the northwest tip of T1 (see insert in Figs. 1, 10 and 11).

5.3. Mechanics of the trench–trench (TT) interaction

Our observations suggest that, to accommodate the subduction of the SCS, T1 propagated over several hundreds kilometers, first westward probably along the COB, and then northwestward within the continental lithosphere of the EUR plate (Fig. 9). Strong deformation is expected near the intersection between T1 and the western edge of the PSP, i.e. the northern Luzon volcanic arc, as presently attested by the concentration of seismic activity (Fig. 7). Parts of the northern Luzon volcanic arc could have been offscrapped during its oblique subduction at several locations marked by forearc basement rises between 125 and 126°E (Hsu et al., 1996) or east of 122°E (Cheng et al., 1996; Font et al., 2001).

The SCS slab is apparently detaching at shallow depths beneath central Taiwan. The detachment D2 trends parallel to the flexure of the EUR plate whereas the COB of the EUR plate should trend obliquely if it follows the general trend of the northern margin of the SCS (Figs. 1 and 10). The high heat-flow ($>240\ mW/m^2$) measured in the Central Range (Lee and Cheng, 1986) could result from asthenospheric flow through D2. We must admit that we have poor constraints on the trend of the subducting COB. Its trace can be significantly different with a virgation toward the north and an intersection with the northern edge of the subducting SCS closer to Taiwan. In general, slab detachments parallel the strike of the trench–arc systems (see D1 for example, Fig. 6a), because they initiate along the area of maximum bending where the lithosphere is the weakest. Detachment could reflect and accommodate the flip of subduction polarity from one side of Taiwan to the other as proposed by Chemenda et al. (1997, 2001). Slab breakoff allowing the flip in the subduction polarity beneath Taiwan was also proposed by Teng et al. (2000), who initiate the detachment within the EUR plate earlier and further northeast beneath the SOT. In their model, a large piece of the EUR slab should sink beneath the southern Ryukyu Trench, which is not supported by our tomographic sections. In other words, the buoyant EUR lithosphere stopped to subduct eastward beneath the Taiwan western foothills and a westward subduction of the Huatung Basin (PSP) is just initiating offshore northern Taiwan, propagating to the south. This scenario could also explain the absence of historical seismicity at the northwestern tip of T1.

The EUR plate steepens rapidly after subduction beneath central Taiwan because it strongly interacts with the PSP to the north (insert of Fig. 10). Furthermore, PSP slab pull is required to produce extension within the Ryukyu arc and to authorize the rifting of the SOT.

What are the driving forces that allow the PSP to migrate through the EUR continent? Obviously, the PSP should encounter strong resistive forces from the EUR lithosphere as attested by the intense seismic activity, plate contorsion and supposed failure in the vicinity of the 'slab–continent collision' beneath northern Taiwan. We see two main forces that could be responsible for the failure of the EUR plate along T1 and the lateral migration of the PSP. They are the slab pull exerted by both the SCS and the PSP lithospheres and the plate kinematics that provides the geodynamic context for such propagation. Indeed, it has been shown by Pacanovsky et al. (1999) that slab pull forces are dominant in determining the stress state of the PSP, even if collisional forces could be locally twice larger.

5.4. Timing of the tectonic events

The present-day kinematics of the PSP is well constrained now from recent GPS measurements (Yu et al., 1997, 1999), but is uncertain for the past because it is entirely surrounded by subduction zones. The present pole of rotation of the PSP with respect to EUR, northeast of Hokkaido (Japan), is generally accepted for the last few millions of years. Some authors invoke a change of the pole 3 Ma ago or earlier allowing a more northward motion of the PSP in the past. Such northward motion for most of the tertiary time is also required to fit paleomagnetic data. Hall et al. (1995), for example, argue that rotation about the present pole cannot account for the observed inclination shifts before 5 Ma as all result in relatively small changes in latitude. Huchon (1985) or Barrier and Angelier (1986) and others, based on regional stress field, favored a change between 3 and 5 Ma. This change, based on regional stress field in Japan and Taiwan, is now debated because the relationship between the stress field along an active margin and the direction of convergence is not clear where arc–continent collision occurs. The stress field also depends on the shape of the indenter (Izu–Bonin Arc or Chinese platform).

Arc volcanism along the northern Luzon Arc was recorded continuously since 17 Ma with short occurrences around 25 and 30 Ma (see Section 2.2) which means that subduction occurred along this arc since at least 17 Ma. Detailed marine studies north of Luzon indicate that subduction necessarily occurred along the Manila Trench in the past because no paleotrench was found on the east side of the arc (e.g. Lewis and Hayes, 1983). Subduction beneath

the central Ryukyu Arc is attested by arc volcanism since at least 18 Ma, whereas it began only 2.8 Ma ago in the southernmost Ryukyu Arc (see Section 2.1). Rifting of the SOT results from a pull force exerted by the PSP slab, which means that the slab might exist, and according to arc volcanism records, it did not existed prior to 2.8 Ma. We have seen that the present subducting plate is old (Early Cretaceous) and thus dense enough to generate a significant slab pull force. Assuming that the SOT opened at the present rate of 40 km/Ma, 2 Ma are needed to create the basin (Lallemand and Liu, 1998).

The southernmost Ryukyu islands (from Yonaguni to Miyako on Fig. 1) just emerged during Holocene as attested by the widespread distribution of the Late Pleistocene Ryukyu reef limestone on all the islands (Kizaki, 1986; Miki, 1995). Fabbri and Fournier (1999), based on a microtectonic study on these islands, concluded that the stress field changed during the Miocene from an intermediate-type to an extensional one in a NNW–SSE direction until Holocene time. Then, it changed again for an arc-perpendicular (N–S) direction of extension recorded on Yonaguni and an arc-parallel (ENE–WSW) direction of extension in Miyako Island. These sedimentological and tectonic observations may be correlated with the initiation and activity of T1 and the associated propagating subduction of the PSP.

Detachment D2 suspected in the EUR slab should took place recently because it is observed at about 70 km depth. Assuming a convergence rate of 7 cm/yr in the direction N100° (normal to D2) and a plate interface dipping 30° toward N100° beneath the Central Range, we obtain 4 cm/yr for the descending rate of the EUR slab. Considering that slab breakoff unlikely occurred at depths shallower than 30 km, we conclude that D2 initiated less than 1 Ma ago with a younger age toward the south because of its propagation.

6. Evolution of the plate boundaries from Japan to Luzon during the last 10 my

Finally, we aim to test the validity of our reconstruction (Fig. 10) by backtracking the PSP with respect to the EUR plate (South China Block in fact) from its present location to the situation 10 Ma ago (Fig. 12). We simply assume that the direction of plate convergence did not changed significantly during the last 10 my. We thus use the same convergence vector than present, i.e. 80 km/Ma in a N306° azimuth near Taiwan. By doing this, we probably make an error in the timing of the events, but the error should be small. Indeed, arc volcanism indicates that subduction was active along the N–S trending Luzon Arc since at least 17 Ma, which means that the convergence vector had a significant westward component during that period of time.

The different stages of reconstruction (Fig. 12) were obtained by backtracking the PSP toward the southeast, by 160 km every 2 my, from the fixed EUR. The shape of the subducted parts of both plates come from our estimates based on tomographic sections (Fig. 6). We observe that the initiation of T1 through the EUR plate started at 8 Ma south of Miyako Island, along the continent–ocean transition (COB). T1 then propagated into the EUR continental part from about 4 ± 1 Ma ago. There is some uncertainty due to the poor constraints on the trace of the COB within the EUR (SCS) slab and to the azimuth and rate of the convergence vector at that time. Rifting and opening of the SOT probably started to the east (near 125°E) and propagated to the west after the development of the new subduction zone and as soon as the conditions for the slab retreat were fulfilled. Such conditions were probably reached around 2 ± 1 Ma ago depending on the longitude. The detachment of the PSP beneath central and northern Ryukyu Arc (D1) probably occurred 3–5 my ago, because it was located just beneath the Ryukyu Arc at that time, at the place where the bending of the plate was maximum. Slab detachment could have occurred along the boundary between an Early Cretaceous basin (old and dense) and an Eocene one (younger and thus less dense). We observe that 3 Ma is close to the age of the change in the propagation direction of T1 as well as the age proposed by several authors for a change in the stress field in Japan and Taiwan.

Before 8 Ma ago, we envisage two hypotheses (see Fig. 12):

*Hyp.*1: the relative motion between the plates is the same. In this case, the PSP has to extend toward the northwest (see question marks on Fig. 6a). If not, there is a gap (small triangle with a dashed line) between both plates. A NW–SE transform thus connected the

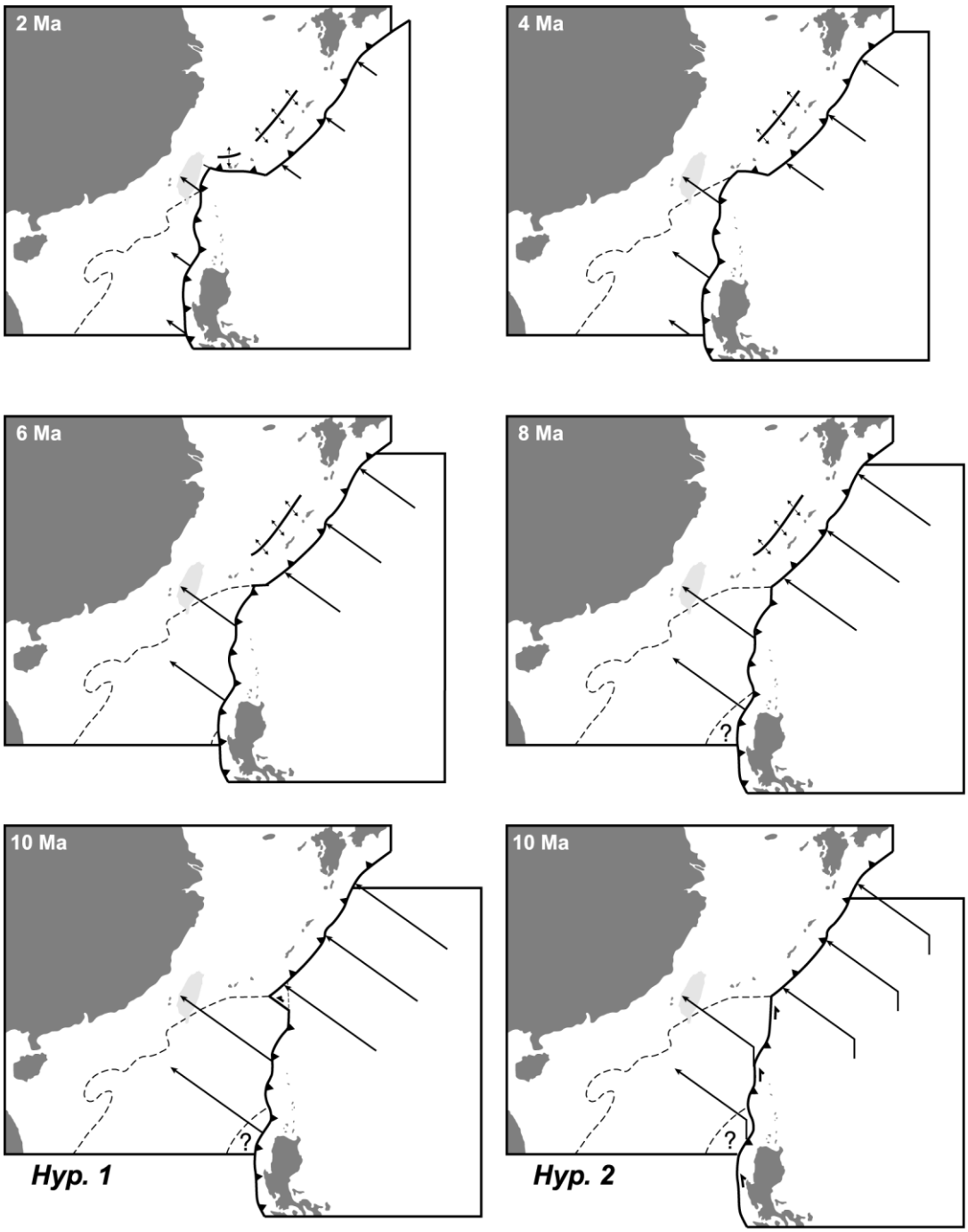

Fig. 12. Plate reconstruction of the boundary between EUR and PSP during the last 10 my. We have made the simple assumption that the PSP moved in the same direction and at the same rate with respect to EUR than today, except before 8 Ma ago where a second hypothesis (Hyp. 2) of northward motion of the PSP is tested. In this simple reconstruction, we have considered that no internal deformation occurred within the PSP, so that the northern Luzon Arc remains N–S trending. Consequently, the second hypothesis (Hyp. 2) contradicts the occurrence of arc magmatism along the northern Luzon Arc. Hyp. 2 is also not compatible with the NW extent of the subducted PSP (see details in the text).

opposite verging subduction zones and subduction was active along the central and northern Ryukyu Arc as well as the northern Luzon Arc prior to 8 Ma. Many authors have suggested that a transform zone connected both trenches in the past.

*Hyp.*2: the relative motion between the plates was N–S prior to 8 Ma ago. In this case, the western edge of the subducted PSP must trend N–S (see question marks on Fig. 6a). The major problem with this second hypothesis is the very high obliquity of convergence (even transform along some segments) along the Manila Trench, which seems not compatible with arc volcanism observed all over this period of time. We thus favor Hyp.1.

Depending on the changes in the azimuth and rate of the convergence, the age of the various tectonic events may change, but we are confident that the shape of the subducted part of the plates, estimated from tomography, as well as the activity of arc volcanism provide solid constraints to our model. Le Pichon (pers. comm., 1997) also mentioned a change in EUR/PSP rotation pole at 8 Ma as well as the existence of a major N–S shear zone that crossed the Ryukyu Arc just east of Miyako. This dextral shear zone was active during the opening of the Japan Sea which ended around 15 Ma ago. About 230 km of dextral slip might be responsible for the change of strike of the Ryukyu margin near Miyako. Our study also confirms the reconstruction proposed by Rangin et al. (1990), in which the SCS extended toward the NE, the southern Ryukyu Trench did not exist prior to a few Ma ago, and a transform zone connected both trenches at that time.

7. Consequences of our model and conclusions

Our model indicates that:

- The southern Ryukyu Arc was not a subduction zone prior to about 8 Ma. It was in the position of the northern passive margin of the SCS.
- The northern Luzon volcanic arc extended about 400 km north of Hualien. It is now subducted beneath and should be partly offscraped in front of the southern Ryukyu Arc.
- The EUR plate teared along T1 as soon as the transform fault connecting both trenches was consumed, i.e. about 8 Ma ago. At that time, the northernmost Luzon volcanic arc has collided with the passive margin of the SCS. It corresponds to the first unconformity described in the Western Foothills of Taiwan by Chang and Chi (1983).
- T1 first propagated along the continent–ocean transition (COB), so that only the oceanic part of EUR was subducting beneath the northern Luzon Arc. The collision was thus mainly restricted to the frontal part of the southern Ryukyu Arc between Miyako and Ishigaki islands.
- A major tectonic event occurred between 3 and 5 my ago with the detachment of the PSP slab beneath the central and northern Ryukyu Arc and subsequent changes in the stress field of Japan and Taiwan and in the direction of propagation of T1 from E–W to NW–SE. Such detachment could have been caused by the subduction/collision of buoyant features such as the Palau–Kyushu Ridge and the Amami Plateau.
- This change in the trend of T1 allowed the continental part of EUR plate to subduct beneath the PSP. It marked the onset of mountain building in Taiwan as a direct response of continental subduction. 3 Ma corresponds to the second unconformity found in the Western Foothills of Taiwan (Chang and Chi, 1983).
- Rifting of the SOT probably started 3 Ma ago north of Miyako and propagated westward during the Quaternary, as a consequence of the slab pull exerted by the PSP slab. Such slab pull is explained by the old age of the slab in this area (about 130 Ma according to Deschamps et al., 2000) and its length (more than 600 km according to tomographic sections).
- Because of the obliquity of the COB with respect to T1, an increasing width of continent is subducting beneath the oceanic PSP, so that T1 has now stopped to propagate into the continent. The EUR slab started to detach from north to south beneath the Central Range of Taiwan 1 Ma ago, allowing a new subduction zone to initiate beneath northeastern Taiwan. Such flip of the subduction polarity may be the forewarning of an eventual connection between the Ryukyu and Philippine trenches and the cessation of the subduction along the Manila Trench.

There are also several consequences in terms of

magmatism along the arcs that need to be examined in the future. Other kinematic scenarii could also be explored allowing more deformation of the PSP near Luzon as suggested by many authors (e.g. Lewis and Hayes, 1983; Lee and Lawver, 1995) but we need first to get more geological constraints.

An important conclusion is undoubtedly the discovery of a rare process of trench lateral migration along a tear that propagates into another plate.

Acknowledgements

We deeply thank Anne Delplanque for her generous help in the drawings. This study greatly benefited from discussions with Anne Deschamps, Frédéric Masson, Francis Wu, Jacques Malavieille, Cheng-Horng Lin and many other colleagues. Dapeng Zhao, Jean-Pierre Burg and an anonymous reviewer are also thanked for their constructive remarks. This is a contribution to the France–Taiwan cooperation program supported by the French Institute in Taipei and the National Science Council of Taiwan.

References

Angelier, J., 1986. Geodynamics of Eurasia–Philippine Sea plate boundary: Preface. Tectonophysics 125, IX–X.

Angelier, J., Barrier, E., Chu, H.T., 1986. Plate collision and paleostress trajectories in a fold-thrust belt: the foothills of Taiwan. Tectonophysics 125, 161–178.

Angelier, J., Chu, H.-T., Lee, J.-C., 1997. Shear concentration in a collision zone: kinematics of the Chihshang Fault as revealed by outcrop-scale quantification of active faulting. Tectonophysics 1–3, 117–144.

Barrier, E., 1985. Un grand accident actif: la faille de la vallée longitudinale de Taïwan (Taïwan République de Chine). Rev. Géol. Dyn. Géogr. Phys. 26 (1), 43–58.

Barrier, E., Angelier, J., 1986. Active collision in eastern Taiwan: the coastal range. Tectonophysics 125, 39–72.

Bijwaard, H., Spakman, W., Engdahl, R., 1998. Closing the gap between regional and global travel time tomography. J. Geophys. Res. 103, 30055–30078.

Chamot-Rooke, N., Le Pichon, X., 1999. GPS determined eastward Sundaland motion with respect to Eurasia confirmed by earthquakes slip vectors at Sunda and Philippine trenches. Earth Planet. Sci. Lett. 173 (99), 439–455.

Chang, S.-L., Chi, W.R., 1983. Neogene nanoplankton biostratigraphy in Taiwan and the tectonic implications. Petrol. Geol. Taiwan 19, 93–147.

Chemenda, A., Yang, R.-K., Hsieh, C.-H., Groholsky, A.L., 1997. Evolutionary model for the Taiwan collision based on physical modelling. Tectonophysics 1–3, 253–274.

Chemenda, A.I., Yang, R.-K., Stéphan, J.-F., Konstantinovskaya, E.A., Ivanov, G.M., 2001. New results from physical modelling of arc–continent collision in Taiwan: evolutionary model. Tectonophysics 33 (1–2), 159–178.

Chen, Y.-L., 1995. Three-dimensional velocity structure and kinematic analysis in Taiwan area. MS thesis, National Central University, Chung-Li, 172 pp.

Cheng, W.-B., Wang, C., Shyu, C.-T., 1996. Crustal structure of the northeastern Taiwan area from seismic refraction data and its tectonic implications. Terr. Atm. Ocean. Sci. 7 (4), 467–487.

Deffontaines, B., Lee, J.-C., Angelier, J., Carvalho, J., Rudant, J.-P., 1994. New geomorphic data on the active Taiwan orogen: a multisource approach. J. Geophys. Res. 99, 20243–20266.

Delcaillau, B., Déramond, J., Souquet, P., Angelier, J., Chu, H.-T., Lee, J.-C., Lee, T.-Q., Lee, T.-F., Liew, P.-M., Lin, T.-S., 1994. Enregistrement tectono-sédimentaire de deux collisions dans l'avant-pays nord-occidental de la Chaîne de Taïwan. C.R. Acad. Sci. Paris 318 (II), 985–991.

Deschamps, A., Monié, P., Lallemand, S., Hsu, S.-K., Yeh, J., 2000. Evidence for Early Cretaceous oceanic crust trapped in the Philippine Sea Plate. Earth Planet. Sci. Lett. 179, 503–516.

Dominguez, S., Lallemand, S., Malavieille, J., Schnürle, P., 1998. Oblique subduction of the Gagua Ridge beneath the Ryukyu accretionary wedge system: Insights from marine observations and sandbox experiments. Mar. Geophys. Res. 20 (5), 383–402.

Engdahl, R., van der Hilst, R.D., Buland, R.P., 1998. Global teleseismic earthquake relocation with improved travel times and procedures for depth determination. Bull. Seismol. Soc. Am. 88, 722–743.

Fabbri, O., Fournier, M., 1999. Extension in the southern Ryukyu arc (Japan): link with oblique subduction and backarc rifting. Tectonics 18 (3), 486–497.

Font, Y., Lallemand, S., Angelier, J., 1999. Etude de la transition entre l'orogène actif de Taiwan et la subduction des Ryukyu — Apport de la sismicité. Bull. Soc. Géol. Fr. 170 (3), 271–283.

Font, Y., Liu, C.-S., Schnürle, P., Lallemand, S., 2001. Constraints on backstop geometry from the Southwest Ryukyu Subduction based on reflection seismic data. Tectonophysics 333 (1–2), 135–158.

Hall, R., Ali, J.R., Anderson, C.D., Baker, S.J., 1995. Origin and motion history of the Philippine Sea Plate. Tectonophysics 251, 229–250.

Hsu, S.-K., Sibuet, J.-C., Monti, S., Shyu, C.-T., Liu, C.-S., 1996. Transition between the Okinawa Trough backarc extension and the Taiwan collision: new insights on the southernmost Ryukyu subduction zone. Mar. Geophys. Res. 18, 163–187.

Hsu, S.-K., Liu, C.-S., Shyu, C.-T., Liu, S.-Y., Lallemand, S., Sibuet, J.-C., Wang, C., Reed, D., Karp, B., 1998. New gravity and magnetic anomaly maps in the Taiwan-Luzon region and their preliminary interpretation. Terr. Atmos. Ocean. Sci. 9 (3), 509–532.

Huang, T., 1984. Planktic foraminiferal biostratigraphy and datum planes in the Neogene sedimentary sequence in Taiwan. Palaeogeogr. Palaeoclimatol. Palaeoecol. 46, 97–106.

Huang, C.-Y., Wu, W.-Y., Chang, C.-P., Tsao, S., Yuan, P.B., Lin, C.-W., Kuan-Yuan, X., 1997. Tectonic evolution of accretionary prism in the arc–continent collision terrane of Taiwan. Tectonophysics 281, 31–51.

Huchon, P., 1985. Géodynamique de la zone de collision d'Izu et de la jonction triple du Japon central. Leur place dans l'évolution de la plaque Philippine. Mem. Sci. Terre, Univ. P. & M. Curie 85–86, 414.

Huchon, P., 1986. Comment on kinematics of the Philippine Sea plate. Tectonics 5, 1355–1383.

Imanishi, M., Kimata, F., Inamori, N., Miyajima, R., Okuda, T., Takai, K., Hirahara, K., 1996. Horizontal displacements by GPS measurements at the Okinawa–Sakishima Islands (1994–1995). Earthquake 2 (49), 417–421.

Jolivet, L., Huchon, P., Rangin, C., 1989. Tectonic setting of western Pacific marginal basins. Tectonophysics 160, 23–47.

Juang, W.S., Bellon, H., 1984. The potassium-argon dating of andesites from Taiwan. Proc. Geol. Soc. China 27, 86–100.

Kao, H., Chen, W.-P., 1991. Earthquakes along the Ryukyu–Kyushu Arc: Strain segmentation, lateral compression, and the thermomechanical state of the plate interface. J. Geophys. Res. 96, 21443–21485.

Kao, H., Chen, W.-P., 2000. The Chi-Chi earthquake sequence of 20 September 1999 in Taiwan: seismotectonics of an active, out-of-sequence thrust. Science 288, 2346–2349.

Kao, H., Jian, P.-R., 2001. Seismogenic patterns in the Taiwan region: insights from source parameter inversion of BATS data. Tectonophysics 333 (1–2), 179–198.

Kao, H., Rau, R.-J., 1999. Detailed structures of the subducted Philippine Sea plate beneath northeast Taiwan: a new type of double seismic zone. J. Geophys. Res. 104, 1015–1033.

Kao, H., Shen, S.-J., Ma, K.-F., 1998. Transition from oblique subduction to collision: earthquakes in the southernmost Ryukyu arc — Taiwan region. J. Geophys. Res. 103, 7211–7229.

Kao, H., Huang, G.-C., Liu, C.-S., 2000. Transition from oblique subduction to collision in the northern Luzon arc — Taiwan region: constraints from bathymetry and seismic observations. J. Geophys. Res. 105, 3059–3079.

Katsumata, M., Sykes, L.R., 1969. Seismicity and tectonics of the western Pacific: Izu–Mariana–Caroline and Ryukyu–Taiwan regions. J. Geophys. Res. 74, 5923–5948.

Kirby, S., Engdahl, E.R., Denlinger, R., 1996. Intermediate-depth intraslab earthquakes and arc volcanism as physical expressions of crustal and uppermost mantle metamorphism in subducting slabs. Subduction: Top to Bottom, Geophys. Monogr. 96, AGU 96, 195–214.

Kizaki, K., 1986. Geology and tectonics of the Ryukyu islands. Tectonophysics 125, 193–207.

Lallemand, S., Liu, C.-S., 1998. Geodynamic implications of present-day kinematics in the southern Ryukyus. J. Geol. Soc. China 41 (4), 551–564.

Lallemand, S.E., Liu, C.-S., Font, Y., 1997a. A tear fault boundary between the Taiwan orogen and the Ryukyu subduction zone. Tectonophysics 274 (1–3), 171–190.

Lallemand, S.E., Liu, C.-S., The ACT scientific crew, 1997b. Swath Bathymetry Reveals Active Arc–Continent Collision Near Taiwan. EOS, Trans. AGU 78, 173–175.

Lallemand, S., Liu, C.-S., Dominguez, S., Schnürle, P., Malavieille, J., The ACT scientific crew, 1999. Trench-parallel stretching and folding of forearc basins and lateral migration of the accretionary wedge in the southern Ryukyus: a case of strain partition caused by oblique convergence. Tectonics 18 (2), 231–247.

Lee, C.-R., Cheng, W.T., 1986. Preliminary heat-flow measurements in Taiwan. In: Horn, M.K. (Ed.), Transactions of the Fourth Circum-Pacific Energy and Mineral Resources Conference, Circum-Pacific Energy and Mineral Resources, Tulsa.

Lee, T.-Y., Lawver, L.A., 1995. Cenozoic plate reconstruction of Southeast Asia. Tectonophysics 251, 85–138.

Lee, T.-Q., Kissel, C., Barrier, E., Laj, C., Chi, W.-R., 1991. Paleomagnetic evidence for a diachronic clockwise rotation of the Coastal Range, eastern Taiwan. Earth Planet. Sci. Lett. 104, 245–257.

Lee, J.-C., Angelier, J., Chu, H.-T., Hu, J.-C., Jen, F.-S., 2001. Continuous monitoring of an active fault in a plate suture zone: a creepmeter study of the Chihshang Fault, eastern Taiwan. Tectonophysics 333 (1–2), 219–240.

Lévêque, J.-J., Rivera, L., Wittlinger, G., 1993. On the use of the checker-board test to assess the resolution of tomographic inversions. Geophys. J. Int. 115, 313–318.

Lewis, S.D., Hayes, D.E., 1983. The tectonics of northward propagating subduction along Eastern Luzon, Phlippine Islands. The tectonic and geologic evolution of SE Asian seas and islands: Part II, Hayes, D.E. (Ed.). Geophys. Monogr. 27, AGU, Washington, D.C., 57–78.

Lin, C.H., Roecker, S.W., 1993. Deep earthquakes beneath central Taiwan: mantle shearing in an arc–continent collision. Tectonics 12, 745–755.

Lin, C.-H., Yeh, Y.-H., Yen, H.-Y., Chen, K.-C., Huang, B.-S., Roecker, S.W., Chiu, J.-M., 1998. Three-dimensional elastic wave velocity structure of the Hualien region of Taiwan: Evidence of active crustal exhumation. Tectonics 17 (1), 89–103.

Liu, C.S., Huang, I.L., Teng, L.S., 1997. Structural features off southwestern Taiwan. Marine Geol. 137, 305–319.

Lu, C.Y., Hsü, K.J., 1992. Tectonic evolution of the Taiwan mountain belt. Petrol. Geol. Taiwan 27, 21–46.

Ma, K.-F., Lee, C.-T., Tsai, Y.-B., Shin, T.-C., Mori, J., 1999. The Chi-Chi Taiwan earthquake: large surface displacements on an inland thrust fault. EOS 80 (50), 605 (see also p. 611).

Malavieille, J., Lallemand, S.E., Deschamps, A., Dominguez, S., Lu, C.Y., Liu, C.S., The ACT scientific crew, 1998. Geology of the Arc–continent collision in Taiwan: marine observations and geodynamic models. abstract in AGU Fall Meeting 1998, San Francisco, 6–10, December, 1998. EOS Trans. AGU (Suppl.) 79 (45), 189.

Malavieille, J., Lallemand, S.E., Dominguez, S., Deschamps, A., Lu, C.-Y., Liu, C.-S., Schnürle, P., The ACT scientific crew, 2001. Geology of the arc–continent collision in Taiwan: marine observations and geodynamic model. Geol. Soc. Am. Spec. Paper (in press).

Matsumoto, T., Kimura, M., Fujioka, K., Kato, Y., Aoki, M., 1993. Detailed bottom topography in the southwesternmost part of the Nanseishoto trench area. JAMSTECR 30, 17–36.

McIntosh, K.D., Nakamura, Y., 1998. Crustal structure beneath the Nanao forearc basin from TAICRUST MCS/OBS Line 14. Terr. Atmos. Ocean. Sci. 9 (3), 345–362.

Miki, M., 1995. Two-phase opening model for the Okinawa Trough inferred from paleomagnetic study of the Ryukyu Arc. J. Geophys. Res. 100, 8169–8184.

Mouthereau, F., 2000. Evolution structurale et cinématique récente de l'avant-pays plissé d'une chaîne de collision oblique: Taïwan. PhD thesis, Mém. Sc. Terre Univ. P. et M. Curie, 475pp.

Mouthereau, F., Lacombe, O., Deffontaines, B., Angelier, J., Chu, H.-T., Lee, C.-T., 1999. Quaternary transfer faulting and belt front deformation at Pakuashan (western Taiwan). Tectonics 18 (2), 215–230.

Okino, K., Ohara, Y., Kasuga, S., Kato, Y., 1999. The Philippine Sea: new survey results reveal the structure and the history of the marginal basins. Geophys. Res. Lett. 26 (15), 2287–2290.

Pacanovsky, K.M., Davis, D.M., Richardson, R.M., Coblentz, D.D., 1999. Intraplate stresses and plate-driving forces in the Philippine Sea plate. J. Geophys. Res. 104, 1095–1110.

Park, J.O., Tokuyama, H., Shinohara, M., Suyehiro, K., Taira, A., 1998. Seismic record of tectonic evolution and back-arc rifting in the southern Ryukyu island arc system. Tectonophysics 294, 21–42.

Rangin, C., Jolivet, L., Pubellier, M., The Tethys Pacific working group, 1990. A simple model for the tectonic evolution of southeast Asia and Indonesia region for the past 43 my. Bull. Soc. Géol. Fr. 8 (VI 6), 889–905.

Rangin, C., Spakman, W., Pubellier, M., Bijwaard, H., 1999a. Tomographic and geological constraints on subduction along the eastern Sundaland continental margin (South-East Asia). Bull. Soc. Géol. Fr. 170 (6), 775–788.

Rangin, C., Le Pichon, X., Mazzotti, S., Pubellier, M., Chamot-Rooke, N., Aurelio, M., Walpersdorf, A., Quebral, R., 1999b. Plate convergence measured by GPS across the Sundaland/Philippine Sea Plate deformed boundary: the Philippines and eastern Indonesia. Geophys. J. Int. 139, 296–316.

Rau, R.-J., Wu, F.T., 1995. Tomographic imaging of lithospheric structures under Taiwan. Earth Planet. Sci. Lett. 133, 517–532.

Richard, M., Bellon, H., Maury, R., Barrier, E., Juang, W.S., 1986. Miocene to recent calc-alkalic volcanism in eastern Taiwan: K–Ar ages and petrography. Mem. Geol. Soc. China 7, 369–382.

Seno, T., Maruyama, S., 1984. Paleogeographic reconstruction and origin of the Philippine Sea. Tectonophysics 102, 53–84.

Seno, T., Stein, S., Gripp, A.E., 1993. A model for the motion of the Philippine Sea plate consistent with NUVEL-1 and geologic data. J. Geophys. Res. 98, 17941–17948.

Shimizu, S., Itaya, T., 1993. Plio-Pleistocene arc magmatism controlled by two overlapping subducted plates, central Japan. Tectonophysics 225, 139–154.

Shinjo, R., 1999. Geochemistry of high Mg andesites and the tectonic evolution of the Okinawa Trough — Ryukyu arc system. Chem. Geol. 157, 69–88.

Sibuet, J.-C., Deffontaines, B., Hsu, S.-K., Thareau, N., Le Formal, J.-P., Liu, C.-S., The ACT party, 1998. Okinawa Trough backarc basin: early tectonic and magmatic evolution. J. Geophys. Res. 103, 30245–30267.

Suppe, J., 1981. Mechanics of mountain building and metamorphism in Taiwan. Mem. Geol. Soc. China 4, 67–89.

Suppe, J., 1984. Kinematics of arc–continent collision, flipping of subduction and back-arc spreading near Taiwan. Geol. Soc. China Mem. 6, 131–146.

Taylor, B., Hayes, D.E., 1983. Origin and history of the South China Basin. The tectonic and geologic evolution of SE Asian seas and islands: Part II, Hayes, D.E. (Ed.). Geophys. Monogr. 27, AGU, Washington, D.C., 23–56.

Teng, L.S., 1996. Extensional collapse of the northern Taiwan mountain belt. Geology 24 (10), 949–952.

Teng, L.S., Lee, C.-T., Tsai, Y.-B., Hsiao, L.-Y., 2000. Slab breakoff as a mechanism for flipping of subduction polarity in Taiwan. Geology 28 (2), 155–158.

Tsai, Y.-B., 1986. Seismotectonics of Taiwan. Tectonophysics 125, 17–37.

Wang, T.-K., Chiang, C.-H., 1998. Imaging of arc-arc collision in the Ryukyu forearc region offshore Hualien from TAICRUST OBS Line 16. Terr. Atmos. Ocean. Sci. 9 (3), 329–344.

Wang, K.-L., Chung, S.-L., Chen, C.-H., Shinjo, R., Yang, T.F., Chen, C.-H., 1999. Post-collisional magmatism around northern Taiwan and its relation with opening of the Okinawa Trough. Tectonophysics 308, 363–376.

Wu, F.T., 1978. Recent tectonics of Taïwan. J. Phys. Earth 26, S265–S299.

Wu, F.T., Chen, K.C., Wang, J.H., McCaffrey, R., Salzberg, D., 1989. Focal mechanisms of recent large earthquakes and the nature of faulting in the Longitudinal Valley of eastern Taiwan. Proc. Geol. Soc. China 32, 157–177.

Wu, F., Rau, R.-J., Salzberg, D., 1997. Taiwan orogeny: thin-skinned or lithospheric collision? Tectonophysics 274, 191–220.

Yang, T.F., Tien, J.-L., Chen, C.-H., Lee, T., Punongbayan, R.S., 1995. Fission-track dating of volcanics in the northern part of the Taiwan — Luzon Arc: eruption ages and evidence for crustal contamination. J. Southeast Asian Earth Sci. 11 (2), 81–93.

Yang, T.F., Lee, T., Chen, C.-H., Cheng, S.-N., Knittel, U., Punongbayan, R.S., Rasdas, A.R., 1996. A double island arc between Taiwan and Luzon: consequence of ridge subduction. Tectonophysics 258, 85–101.

Yu, H.-S., Chou, Y.-W., 2001. Characteristics and development of the flexural forebulge and basal unconformity of Western Taiwan foreland basin. Tectonophysics 333 (1–2), 277–291.

Yu, S.-B., Chen, H.-Y., Kuo, L.-C., 1997. Velocity field of GPS stations in the Taiwan area. Tectonophysics 274 (1–3), 41–59.

Yu, S.-B., Kuo, L.-C., Punongbayan, R.S., Ramos, E.G., 1999. GPS observation of crustal deformation in the Taiwan–Luzon region. Geophys. Res. Lett. 26 (7), 923–926.